

**Carbon content of
aerosols from the
burning of biomass**

L. L. Soto-García et al.

This discussion paper is/has been under review for the journal Atmospheric Chemistry and Physics (ACP). Please refer to the corresponding final paper in ACP if available.

Evaluation of the carbon content of aerosols from the burning of biomass in the Brazilian Amazon using thermal, optical and thermal-optical analysis methods

L. L. Soto-García^{1,2}, M. O. Andreae³, T. W. Andreae³, P. Artaxo⁴, W. Maenhaut⁵, T. Kirchstetter⁶, T. Novakov⁶, J. C. Chow⁷, and O. L. Mayol-Bracero¹

¹Institute for Tropical Ecosystem Studies, University of Puerto Rico, San Juan, Puerto Rico

²Department of Chemistry, University of Puerto Rico, San Juan, Puerto Rico

³Biogeochemistry Department, Max Planck Institute for Chemistry, Mainz, Germany

⁴Institute for Physics, University of São Paulo, São Paulo, Brazil

⁵Institute for Nuclear Sciences, Ghent University, Ghent, Belgium

Title Page

Abstract

Introduction

Conclusions

References

Tables

Figures

◀

▶

◀

▶

Back

Close

Full Screen / Esc

Printer-friendly Version

Interactive Discussion



⁶ Lawrence Berkeley National Laboratory, Berkeley, California, USA

⁷ Desert Research Institute, Reno, Nevada, USA

Received: 9 April 2010 – Accepted: 23 April 2010 – Published: 19 May 2010

Correspondence to: O. L. Mayol-Bracero (omayol@ites.upr.edu)

Published by Copernicus Publications on behalf of the European Geosciences Union.

Carbon content of aerosols from the burning of biomass

L. L. Soto-García et al.

Title Page

Abstract

Introduction

Conclusions

References

Tables

Figures



Back

Close

Full Screen / Esc

Printer-friendly Version

Interactive Discussion



Abstract

Aerosol samples were collected at a pasture site in the Amazon Basin as part of the project LBA-SMOCC-2002 (*Large-Scale Biosphere-Atmosphere Experiment in Amazonia – Smoke Aerosols, Clouds, Rainfall and Climate: Aerosols from Biomass Burning Perturb Global and Regional Climate*). Sampling was conducted during the late dry season, when the aerosol composition was dominated by biomass burning emissions, especially in the submicron fraction. A 13-stage Dekati low-pressure impactor (DLPI) was used to collect particles with nominal aerodynamic diameters ranging from 0.03 to 0.10 μm . Gravimetric analyses of the DLPI substrates and filters were performed to obtain aerosol mass concentrations. The concentrations of total, apparent elemental, and organic carbon (TC, EC_a, and OC) were determined using thermal and thermal-optical analysis (TOA) methods. A light transmission method (LTM) was used to determine the concentration of equivalent black carbon (BC_e) or the absorbing fraction at 880 nm for the size-resolved samples.

During the dry period, due to the pervasive presence of fires in the region upwind of the sampling site, concentrations of fine aerosols ($D_p < 2.5 \mu\text{m}$: average $59.8 \mu\text{g m}^{-3}$) were higher than coarse aerosols ($D_p > 2.5 \mu\text{m}$: $4.1 \mu\text{g m}^{-3}$). Carbonaceous matter, estimated as the sum of the particulate organic matter (i.e., $\text{OC} \times 1.8$) plus BC_e, comprised more than 90% to the total aerosol mass. Concentrations of EC_a (estimated by thermal analysis with a correction for charring) and BC_e (estimated by LTM) averaged 5.2 ± 1.3 and $3.1 \pm 0.8 \mu\text{g m}^{-3}$, respectively. The determination of EC was improved by extracting water soluble organic material from the samples, which reduced the average light absorption Ångström exponent of particles in the size range of 0.1 to 1.0 μm from being greater than 2.0 to approximately 1.2. The size-resolved BC_e measured by the LTM showed a clear maximum between 0.4 to 0.6 μm in diameter. The concentrations of OC and BC_e varied diurnally during the dry period, and this variation is related to diurnal changes in boundary layer thickness and in fire frequency.

Carbon content of aerosols from the burning of biomass

L. L. Soto-García et al.

Title Page

Abstract

Introduction

Conclusions

References

Tables

Figures

◀

▶

◀

▶

Back

Close

Full Screen / Esc

Printer-friendly Version

Interactive Discussion



1 Introduction

Biomass burning in the tropics introduces huge amounts (up to $40\,000\text{ cm}^{-3}$) of aerosol particles into the atmosphere (Artaxo et al., 2002). These particles significantly affect climate forcing (Hobbs et al., 1997), cloud properties and precipitation patterns (Rosenfeld, 1999; Andreae et al., 2004; Koren et al., 2004; Rosenfeld et al., 2008), health (EPA, 2003; Pope and Dockery, 2006), and ecosystems (Barth et al., 2005). The impacts of these particles depend in great part on aerosol composition and size. Therefore, detailed information on their chemical and physical properties is required.

Particles from biomass burning consist mainly of carbonaceous material (elemental carbon (EC or BC), organic carbon (OC)), and a small amount of inorganic material (Reid et al., 2005; Andreae and Gelencsér, 2006; Fuzzi et al., 2007). In the Brazilian Amazon, the chemical composition of the inorganic fraction during biomass burning has been extensively studied (Artaxo et al., 1998, 2000, 2002; Andreae et al., 1997; Reid et al., 1998; Formenti et al., 2003); however, there are relatively few studies focusing on the carbonaceous fraction (Graham et al., 2002; Mayol-Bracero et al., 2002a; Guyon et al., 2003; Falkovich et al., 2005; Decesari et al., 2006; Fuzzi et al., 2007). Findings from the *European contribution to the Large-Scale Biosphere-Atmosphere Experiment in Amazonia* (LBA-EUSTACH) (Andreae et al., 2002; Graham et al., 2002; Mayol-Bracero et al., 2002a) demonstrated that aerosols were predominantly in the fine fraction (accumulation mode particles) (Artaxo et al., 2002) and that most of the carbonaceous material was water-soluble organic carbon (WSOC) (45%–75% of the OC). These findings suggested that this aerosol fraction may contribute significantly to the cloud condensation nuclei (CCN) activity (Mayol-Bracero et al., 2002a). It was also shown that polycarboxylic acids and probably HULIS (humic-like substances) may be responsible for at least 26% of the WSOC fraction (Mayol-Bracero et al., 2002a). The polycarboxylic acid water-soluble fraction is effective at lowering the surface tension of cloud droplets, implying that these compounds might play an important role in the precipitation mechanisms in regions where biomass burning contributes significantly

Carbon content of aerosols from the burning of biomass

L. L. Soto-García et al.

Title Page

Abstract

Introduction

Conclusions

References

Tables

Figures

◀

▶

◀

▶

Back

Close

Full Screen / Esc

Printer-friendly Version

Interactive Discussion



to the total aerosol mass (Mayol-Bracero et al., 2002a; Mircea et al., 2005). During the LBA-SMOCC campaign, Hoffer et al. (2006b) characterized the total carbon (TC) and WSOC from fine bulk samples in order to measure the high-molecular weight carbon (HMWC) compounds. They found that the HMWC dominated the TC composition.

5 Diel variations in anhydrosugars and phenolic acids determined by using GC-MS suggested that the phenolic acids may undergo chemical transformations towards more refractory compounds, as was also implied previously for HULIS.

The majority of these previous investigations have concentrated on characterizing bulk aerosol samples. There are very few studies that present size-resolved information about the carbonaceous fraction during biomass burning at tropical locations. Herckes et al. (2006) reported OC and molecular source marker species size distributions from biomass burning at the Yosemite National Park, CA. This study showed that more than 75% of the OC mass and most of the molecular marker species were associated with fine aerosol particles. Falkovich et al. (2005) studied the low-molecular-weight (LMW) organic acids in aerosol particles using a cascade impactor with eleven stages (Micro Orifice Uniform Deposit Impactor – MOUDI) during LBA-SMOCC. They found that LMW polar organic acids, which may contribute to the CCN activity, accounted for a significant fraction of the WSOC in biomass burning aerosols (10–20%). Also, Fuzzi et al. (2007), during the same campaign, presented an overview of the size-segregated inorganic and organic results from different cascade impactor samplers. This study characterized organic material (mainly water-soluble), ions, and mineral dust. During the dry period, the average mass concentration of particulate matter with a diameter below 10 μm (PM_{10}) was above 50 $\mu\text{g m}^{-3}$. The size distributions were dominated by the fine mode, which was mainly composed of organic material, mostly water-soluble, and had ~10% soluble inorganic salts, with sulfate as the major anion. Decesari et al. (2006) employed different techniques for individual compound analysis in order to speciate the aerosol organic compounds during LBA-SMOCC. In that study, up to 8% of the submicron TC (and 11% of WSOC) was speciated at the molecular level. Polyhydroxylated compounds, aliphatic and aromatic acids were the main classes. Char-

Carbon content of aerosols from the burning of biomass

L. L. Soto-García et al.

Title Page

Abstract

Introduction

Conclusions

References

Tables

Figures

◀

▶

◀

▶

Back

Close

Full Screen / Esc

Printer-friendly Version

Interactive Discussion



acterizations of 50–90% of the WSOC into neutral species, light acids, and humic-like substances were also made. The size-segregated composition of WSOC was summarized by a set of model compounds, which represents both the organic compound composition and the functional groups of the WSOC. With this information one was able to predict the aerosol hygroscopic properties and CCN ability over Amazonia (Mircea et al., 2005).

To our knowledge, a study presenting the size-resolved carbonaceous components (i.e., OC and EC) of biomass-burning dominated aerosols in the Amazon Basin has not been reported. One of the reasons for this is the difficulty in distinguishing OC from EC in biomass burning samples using the commonly used thermal analytical techniques (Gundel et al., 1984; Novakov and Corrigan, 1995; Mayol-Bracero et al., 2002a; Pöschl, 2003; Andreae and Gelencsér, 2006).

Thermal analyses of the carbonaceous fraction from aerosol samples allow the determination of OC and EC_a. Apparent elemental carbon (EC_a) is operationally defined as the fraction of carbon that is oxidized above a certain temperature threshold in the presence of an oxygen-containing atmosphere (Andreae and Gelencsér, 2006). Various corrections for charring are usually made, depending on the specific technique used (Chow et al., 1993, 2001, 2004, 2007; NIOSH, 1996, 1999; Zhen et al., 2002). OC is defined as, TC minus the sum of carbonate and EC_a. A related parameter, equivalent black carbon (BC_e) is defined as the amount of strongly light-absorbing carbon with the approximate optical properties of C_{soot} that would give the same signal in an optical instrument (e.g., in the light transmission method) as the sample. These definitions of EC_a and BC_e are operational and method dependent, and are used as approximations for the concentration of light absorbing carbon (LAC) or soot carbon (C_{soot}) (Andreae and Gelencsér, 2006). C_{soot} refers to carbon particles with the morphological and chemical properties typical of soot particles from combustion: aggregates of spherules made of graphene layers, consisting almost purely of carbon, with minor amounts of bound hetero-elements, especially hydrogen and oxygen. This definition does not include the organic substances (oils, etc.) frequently present in, or on,

Carbon content of aerosols from the burning of biomass

L. L. Soto-García et al.

Title Page

Abstract

Introduction

Conclusions

References

Tables

Figures

◀

▶

◀

▶

Back

Close

Full Screen / Esc

Printer-friendly Version

Interactive Discussion



combustion particles. Together with light-absorbing organic compounds (also called “brown carbon”), C_{soot} makes up the LAC fraction of the atmospheric aerosol.

For biomass burning samples, there is no real sharp boundary for differentiating OC from EC_a , due to the presence of OC material that is highly refractory and optically absorbing, like brown carbon and humic-like substances (Pöschl, 2003; Hoffer et al., 2006a, b; Andreae and Gelencsér, 2006). The results obtained by different authors and different techniques can therefore vary dramatically, especially for EC_a , as a result of different analytical protocols (Novakov and Corrigan, 1995; Mayol-Bracero et al., 2002a; Kirchstetter et al., 2003; Watson et al., 2005).

In this paper, we present the size-resolved concentrations of carbonaceous aerosol particles collected at a pasture site in Rondônia, Brazil, during the biomass-burning dominated part of the LBA-SMOCC campaign (2002), giving special attention to the determination of EC_a or BC_e using several thermal and optical methods.

2 Experimental

2.1 Sampling site and experimental setup

The sampling site was located on a pasture of the ranch Fazenda Nossa Senhora Apareci-da (FNS) in the Brazilian Amazon ($10^{\circ}45'44''$ S, $62^{\circ}21'27''$ W) near the town of Ouro Preto D'Oeste, Rondônia, Brazil. Sample collection took place during the September–October 2002 burning period. This site has experienced intense deforestation by vegetation fires over the last 30 years (since 1977) (Andreae et al., 2002; Kirkman et al., 2002; Trebs et al., 2005).

2.1.1 Dekati low-pressure impactor

Aerosol samples were collected with a 13-stage Dekati low-pressure impactor (DLPI) which separates particles according to their particle diameter (D_p) (from $\sim 10 \mu\text{m}$ down

Carbon content of aerosols from the burning of biomass

L. L. Soto-García et al.

Title Page

Abstract

Introduction

Conclusions

References

Tables

Figures

◀

▶

◀

▶

Back

Close

Full Screen / Esc

Printer-friendly Version

Interactive Discussion



Carbon content of aerosols from the burning of biomass

L. L. Soto-García et al.

Title Page

Abstract

Introduction

Conclusions

References

Tables

Figures

◀

▶

◀

▶

Back

Close

Full Screen / Esc

Printer-friendly Version

Interactive Discussion



to 30 nm). The DLPI was placed on a tower at a height of ~ 8 m. Size-resolved particles were collected on quartz fiber filters (Pallflex Membrane Filter-Tissuquartz 2500 QAT-UP) and Teflon filters (Pall TefloTM– $3.0\ \mu\text{m}$) and on aluminum substrates (MSP Corporation-aluminum foil impaction substrates, 2 mask, MDI-225). One half of each substrate was analyzed using evolved gas analysis (EGA) and the other half using ion chromatography (IC) and/or inductively coupled plasma (ICP) with optical emission spectroscopy (OES). Samples were collected during day and/or night for 12 or 24 h. The sampling flow averaged $29\ \text{L}\ \text{min}^{-1}$ and the pressure 250 hPa. The apparent size range collected on each stage was calculated depending on the DLPI pressure and flow. Size biases resulting from the use of non-standard substrate materials are discussed in Sect. 5.1. Sampled volumes averaged $\sim 16\ \text{m}^3$ and $36\ \text{m}^3$, respectively, and these were converted to standard temperature ($25\ ^\circ\text{C}$) and pressure (1000 hPa).

Blanks were collected using quartz fiber and aluminum substrates on the DLPI sampler in the same way as real samples were taken, with flow being applied only for about 5 s. It should be noted that 5 s is too short a time to represent passive vapor adsorption (Watson et al., 2009). The quartz fiber filters were pre-baked at $600\ ^\circ\text{C}$ for about 15 hours to remove residual organic impurities. After collecting the samples, they were stored in a freezer at $-18\ ^\circ\text{C}$ in Petrislide dishes (Millipore, 47 mm Petrislide, PD1504700) until analysis. Handling of filters was according to the procedures recommended by Salmon et al. (1998) and Mayol-Bracero et al. (2002a). Correction for positive artifacts (overestimation of carbonaceous particle concentration due to adsorption of organic gases to the quartz filters) was not possible in this study due to the use of an impactor sampler.

In Sect. 3 we compare the results obtained with 1) the DLPI used by UPR, 2) a low-volume $\text{PM}_{2.5}$ filter sampler used by Ghent University (R2.5WW UGent) for which the air volume was measured with a calibrated gas meter, 3) three high-volume dichotomous samplers (HVDS), 4) a carbon monitor used by the University of São Paulo (USP), and 5) a 7-wavelength aethalometer from USP, all located at FNS during the SMOCC experiment. Two of the HVDSs were used by UGent (Decesari et al., 2006)

and the other by the Max Planck Institute for Chemistry (MPIC) (Hoffer et al., 2006b). A brief description of these systems is presented below.

2.1.2 Low-volume PM_{2.5} filter sampler (R2.5WW) and High-Volume Dichotomous Samplers (HVDS)

5 The low-volume PM_{2.5} filter sampler (R2.5WW) is a filter holder with 47-mm diameter filters; it was equipped with a Rupprecht & Patashnick PM_{2.5} inlet and operated at a flow rate of 17 L min⁻¹; the face velocity was 22 cm s⁻¹. The HVDS is a system that separates bulk particles into fine ($D_p < \sim 2.5 \mu\text{m}$) and coarse ($D_p > \sim 2.5 \mu\text{m}$) (Solomon et al., 1983). The filter diameter was 102 mm with a face velocity of about 86 cm s⁻¹ for a total average flow of about 330 L min⁻¹. The sampling periods were 12 h during day
10 time, and 12 h during night time during the dry period. Samples were collected with quartz fiber filters (Whatman QM-A for the R2.5WW, Gelman Pall for the HVDS), pre-baked for at least 10 h at 600 °C. In both the R2.5WW and the HVDS, two quartz fiber filters were placed in the filter holders in tandem in order to correct for the adsorption
15 of gaseous organic compounds by the filter material (i.e., positive artifact).

2.1.3 Carbon monitor and aethalometer

The carbon monitor (Model 5400, Rupprecht & Patashnick, Inc.) is an on-line instrument that collects ambient air particles by impaction in order to make hourly measurements of carbonaceous aerosol components (TC, OC, and EC_a). The OC component
20 is the carbon content burned off when a controlled combustion at 350 °C is applied. TC is obtained by combusting the aerosol at 700 °C, and EC_a is derived as the difference between TC and OC (Artaxo et al., 2002). Since aerosols were collected with by impaction, particles smaller than 70 nm may not have been collected efficiently. Because the impaction surfaces were not coated, bounce-off from the impaction surface could
25 have occurred for dry periods.

The aethalometer (AE30, Magee Scientific) is also an on-line device, used to mea-

Carbon content of aerosols from the burning of biomass

L. L. Soto-García et al.

Title Page

Abstract

Introduction

Conclusions

References

Tables

Figures

◀

▶

◀

▶

Back

Close

Full Screen / Esc

Printer-friendly Version

Interactive Discussion



sure equivalent black carbon (BC_e). It was operated with a 5-min time resolution, and an absorption cross section of $10 \text{ m}^2 \text{ g}^{-1}$ was used to convert optical absorption to BC_e (Park et al., 2006). Absorption measurements from the aethalometer agreed well with Nuclepore filter based measurements using a calibrated black carbon standard (Martins et al., 1998a, b). Results from the aethalometer also agreed within 30% with a Multi Angle Absorption Photometer instrument, taking into account the different wavelengths used (Hansen et al., 1984; Schmid et al., 2006).

2.2 Aerosol mass concentration

The mass collected on the aluminum substrates was determined by gravimetric analysis which involved weighing the aluminum substrates before and after sampling, using a Mettler MT5 microbalance ($1 \mu\text{g}$ sensitivity), in a room with stabilized temperature (20°C) and relative humidity (50%). For more details see Hitzenberger et al. (2004).

2.3 Chemical analyses

The analyses presented here are for the bulk and the size-resolved concentrations of carbonaceous components. These concentrations were determined for sections of the low-volume filter sampler, HVDS, DLPI quartz filters and the aluminum substrates, using thermal, thermal optical transmission (TOT) and reflectance (TOR) methods, thermal-optical analysis (TOA), and a light transmission method (LTM). Results from IC and ICP analyses of the inorganic fraction are also included.

2.3.1 Thermal and thermal-optical analysis

A thermal analysis method (evolved gas analysis (EGA)) similar to that described by Novakov (1981) and Kirchstetter et al. (2001) was used at Lawrence Berkeley National Laboratory (LBNL) and MPIC to characterize TC, EC_a and OC. Segments of 0.55 or 1.8 cm^2 were taken from the 3.63 cm^2 exposed area of a 25 mm diameter quartz filter

Carbon content of aerosols from the burning of biomass

L. L. Soto-García et al.

Title Page

Abstract

Introduction

Conclusions

References

Tables

Figures

◀

▶

◀

▶

Back

Close

Full Screen / Esc

Printer-friendly Version

Interactive Discussion



and heated in an oxygen atmosphere at a rate of $\sim 20^\circ\text{C}$ per min from 50°C to $\sim 700^\circ\text{C}$. The evolved carbon was converted to CO_2 over a Pt-coated ceramic (at LBNL) or MnO_2 (at MPIC) catalyst (at 800°C) and measured by a non-dispersive infrared analyzer. Evolved carbon (as CO_2 concentration) was plotted as a function of temperature (i.e., a thermogram). Thermogram peaks indicate carbon volatilization, decomposition, and combustion. The area under the whole thermogram is proportional to the mass of sampled TC. We defined the “apparent elemental carbon” (EC_a) as the portion of the sample evolving above 400°C . OC was calculated using the equation $\text{OC}=\text{TC}-\text{EC}_a$.

To refine the estimate of EC_a , and consequently OC, the intensity of light (at 572 nm) transmitted through the sample was monitored during the thermal analysis. Here we refer to the combination of the thermal and light transmission methods as thermal-optical analysis (TOA). The 572 nm light was generated with a light emitting diode, and the intensity transmitted through the samples was measured with a spectrometer. For additional details see Kirchstetter and Novakov (2007).

Portions of some samples were soaked in 10–15 mL of ultrapurified water for 30 min to extract water-soluble organics and then dried under an infrared lamp prior to analysis.

The thermal method was quantitative for TC to within $\sim 10\%$, with a reproducibility of 5%, and a detection limit of $\sim 0.2\ \mu\text{g}$ per sample (Dod et al., 1979; Gundel et al., 1984). The precision or coefficient of variation (CV) for this method was 4, 6, 4, and 3% for TC, BC, OC, and the BC/OC ratio, respectively (Mayol-Bracero et al., 2002b).

2.3.2 Thermal optical reflectance (TOR) and transmission (TOT) method

TOR and TOT were used at DRI and UGent (only TOT) to also determine the concentration of TC and EC_a . These techniques have been described elsewhere (Chow et al., 1993; Peterson and Richards, 2002; Chen et al., 2004). Briefly, a small sample segment of the filter is taken from a quartz-fiber filter and analyzed. The carbon evolved from the filter is measured with a thermal-optical analyzer, using two heating temperature profiles, one with 100% He and the other with 98% He/2% O_2 . The evolving

Carbon content of aerosols from the burning of biomass

L. L. Soto-García et al.

Title Page

Abstract

Introduction

Conclusions

References

Tables

Figures

◀

▶

◀

▶

Back

Close

Full Screen / Esc

Printer-friendly Version

Interactive Discussion



carbon is oxidized to CO₂, the CO₂ is reduced to CH₄, and the CH₄ is measured using a flame ionization detector. Both methods have a He/Ne laser beam (at 632 nm) that is directed on the filter and the direct forward and/or backward scattering of the radiation is detected by photo-detectors to measure reflectance and transmittance throughout the analysis. This arrangement is used for the correction of the charring effect.

2.3.3 Light Transmission Method (LTM)

Samples collected on quartz fiber filters were analyzed using the light transmission method (LTM) (Kirchstetter et al., 2004). Light attenuation (ATN) was calculated from light transmission through the sample (T): $ATN=100\cdot\ln(1/T)$. In this study, T was defined as $(I_s/I_{s,o}) \cdot (I_{r,o}/I_r)$, where I_s and $I_{s,o}$ are the measured intensities of light transmitted through a quartz fiber filter sample prior to and after removal of carbonaceous material by heating to 700 °C in oxygen, and I_r and $I_{r,o}$ are the intensities of light transmitted through a reference quartz filter measured at the same time as I_s and $I_{s,o}$. I_s and $I_{s,o}$ were measured using the same quartz filter rather than another blank, because light transmission through quartz fiber filters is variable. Measuring $I_{s,o}$ on the same filter also automatically corrects for the absorption due to mineral dust, because light-absorbing dust is not removed during sample heating. In this study, we only wanted to measure aerosol ATN due to carbonaceous material, and not mineral dust.

The reference filter was used to correct for possible instrumental variability such as changes in the brightness of the light source or detector response during the interval between measurements of I_s and $I_{s,o}$. The uncertainty of each measurement when using the LTM was $\sim \pm 2$ units of ATN.

Mass concentrations of BC_e at 880 nm were estimated from LTM data, following the method used for the Aethalometer (Hansen et al., 1984): $BC_e=ATN/\sigma$, where σ is the specific attenuation for BC (19 m² g⁻¹) (Gundel et al., 1984) and ATN is light attenuation at 880 nm by particles on the quartz fiber filters.

Carbon content of aerosols from the burning of biomass

L. L. Soto-García et al.

Title Page

Abstract

Introduction

Conclusions

References

Tables

Figures

◀

▶

◀

▶

Back

Close

Full Screen / Esc

Printer-friendly Version

Interactive Discussion



2.3.4 Ion Chromatography (IC) and Inductively Coupled Plasma (ICP)

Mass concentrations of inorganic species were determined using IC and ICP analysis. Water-soluble ions were determined using isocratic suppressed IC with conductivity detection (DIONEX, Sunnyvale, Ca). The anionic species measured were Cl^- , SO_4^{2-} , and NO_3^- , and the cationic species were NH_4^+ , Ca^{2+} , Mg^{2+} , K^+ , and Na^+ . Filters and substrates were cut in halves and extracted with methanol and/or ultrapure water. ICP together with optical emission spectroscopy (OES) was also used for the determination of trace elements, such as Al, B, Ca, Fe, K, Mg, Mn, Na, Si, and Zn, in the extracted water from the filters and substrates.

3 Results and discussion

Concentrations of carbonaceous species determined by thermal, thermal-optical, and optical analyses are reported in Table 1. From samples analyzed thermally we estimated TC and EC_a concentrations. Samples extracted with water and analyzed using TOA (DLPI #11, 13, and 15) provided TC and EC_w (EC from these analyses is called $\text{EC}_{w572\text{ nm}}$) concentrations. Samples analyzed by the light transmission method (LTM) (DLPI #3, 11, 12, 13, 15, and 25) provided BC_e at 880 nm ($\text{BC}_{e880\text{ nm}}$). Below we explain how these different carbonaceous components were determined.

3.1 Mass and total carbon concentrations

The average fine particle mass concentration for the dry period from 7 September to 7 October was $59.8 (\pm 41.1) \mu\text{g m}^{-3}$, consistent with elevated concentrations reported by Fuzzi et al. (2007). High concentrations were due to the huge areas burning upwind over which the sampled air masses had traveled for several days, and the dynamics of the boundary layer (Fuzzi et al., 2007; Rissler et al., 2006). During the transition period from 7 October to 1 November and the wet period in the first four days of Novem-

Carbon content of aerosols from the burning of biomass

L. L. Soto-García et al.

Title Page

Abstract

Introduction

Conclusions

References

Tables

Figures

◀

▶

◀

▶

Back

Close

Full Screen / Esc

Printer-friendly Version

Interactive Discussion



ber, the average concentrations of the fine fraction were $15.5 (\pm 11.6) \mu\text{g m}^{-3}$ and $3.7 (\pm 1.7) \mu\text{g m}^{-3}$, respectively. The average coarse particle concentration was relatively constant at $4.2 (\pm 2.0) \mu\text{g m}^{-3}$ during the entire period.

TC concentrations in the fine aerosol fraction ranged from 24 to $64 \mu\text{g m}^{-3}$ and averaged $44 \mu\text{g m}^{-3}$ (Table 1). These results are consistent with values from bulk analyses observed at the same site during the dry season in a previous campaign, where TC ranged between 4.4 and $83 \mu\text{g m}^{-3}$ (Graham et al., 2002; Mayol-Bracero et al., 2002a). Similar concentrations were observed in the results from other filter sampling systems during SMOCC, with concentrations ranging from 6.4 to $78.2 \mu\text{g m}^{-3}$ (average $32.7 \mu\text{g m}^{-3}$, HVDS_{UGent}) and 24.9 to $90.9 \mu\text{g m}^{-3}$ (average $51.7 \mu\text{g m}^{-3}$ HVDS_{MPIG}) (Decesari et al., 2006).

The average size-resolved concentrations for total particulate mass and TC are presented in Fig. 1. Both size distributions were bimodal, peaking in the accumulation (0.4–0.6 μm) and coarse modes (1.6–2.4 μm). The average TC/PM ratios from the aluminum substrate samples for the fine and coarse fractions were 0.56 ± 0.08 and 0.31 ± 0.09 , respectively. These results indicate that the carbon content was higher in the fine aerosol fraction than in the coarse fraction. As suggested previously, biogenic and inorganic crustal material might be found in the coarse particles (Fuzzi et al., 2007).

3.2 Light absorbing carbon

Figure 2 presents the size-resolved thermograms from aerosols collected during SMOCC, which were dominated by biomass burning emissions. The thermograms generally had two or three different peaks: peaks below 400°C were attributed to OC and the peak above 400°C corresponded to EC_a, the most refractory material. Concentrations of EC_a averaged $18.1 \mu\text{g m}^{-3}$ in the fine particle mode ($D_p < 2.5 \mu\text{m}$). Uncertainties occurred in the determination of EC_a, especially during biomass burning (Pöschl, 2003; Hoffer et al., 2006a, b; Andreae and Gelencsér, 2006). During

Carbon content of aerosols from the burning of biomass

L. L. Soto-García et al.

Title Page

Abstract

Introduction

Conclusions

References

Tables

Figures

◀

▶

◀

▶

Back

Close

Full Screen / Esc

Printer-friendly Version

Interactive Discussion



the thermal analysis of biomass aerosols, OC in the aerosol surface deposit and in organic vapors adsorbed throughout the filter turned into char as it underwent pyrolysis; this char co-evolves with EC. Also, some highly refractory OC in biomass aerosols co-evolved with EC and might be indistinguishable from it (Hoffer et al., 2006b).

5 In this study, we examined how optical and solvent extraction techniques can be used in addition to thermal analysis to obtain a better estimation of EC in biomass aerosol samples. Figure 3 shows the thermogram from DLPI#11-stage 4 (nominal D_p from 0.2–0.3 μm) before and after extracting with water. Water extraction removed large quantities of OC (~60% for the fine fraction), and the amount of EC_a lost was ~10 50%. For similar samples, Mayol- Bracero et al. (2002a) had found that on average 53% of the EC_a was removed by water extraction. The reduction in EC_a was due to the removal of water-soluble organic compounds and/or the mechanical dislodging of insoluble EC_a . Water extraction resulted in a shift in the evolution of the most refractory material to higher temperatures (the last peak appeared before water extraction at ~450 °C and after water extraction at ~520 °C), most likely because of the removal of water-soluble ions such as K^+ and Na^+ that catalyze the combustion of EC_a (Novakov and Corrigan, 1995; Mayol-Bracero et al., 2002a).

After extraction with water; the single peak above 450° split into two peaks, at ~470 °C and 520 °C. This was observed for all samples with $D_p < 1.6 \mu\text{m}$. These two 20 peaks might be due to different classes of carbonaceous material.

Optical characterization during thermal analysis was also used to determine EC concentrations more accurately. Figure 3 shows light attenuated (at 572 nm) by sample DLPI#11-stage 4 (nominal D_p from 0.2–0.3 μm) throughout the thermal analysis, before ($\text{EC}_{a572 \text{ nm}}$) and after the water extraction ($\text{EC}_{w572 \text{ nm}}$). The point of zero attenuation was used to define the split between OC and $\text{EC}_{a572 \text{ nm}}$ and/or $\text{EC}_{w572 \text{ nm}}$. The 25 formation of char from OC pyrolyzed in the un-extracted sample is evident from the increased attenuation. Relatively little charring was observed in the water extracted sample. Thus, the water soluble material, which can be removed by the extraction technique, was responsible for most of the charring. Concentrations of $\text{EC}_{a572 \text{ nm}}$ and

Carbon content of aerosols from the burning of biomass

L. L. Soto-García et al.

Title Page

Abstract

Introduction

Conclusions

References

Tables

Figures

◀

▶

◀

▶

Back

Close

Full Screen / Esc

Printer-friendly Version

Interactive Discussion



$EC_{w572\text{ nm}}$ were averaged for three samples, and were 5.2 ± 1.3 and $3.2\pm 1.2\ \mu\text{g m}^{-3}$, respectively.

BC_e concentrations ($D_p < 2.5\ \mu\text{m}$) ($BC_{e880\text{ nm}}$) were estimated using LTM only (i.e., not in combination with thermal analysis) and were $3.1\ \mu\text{g m}^{-3}$.

3.3 Comparison of TC, EC and BC concentrations

One problem encountered in the determination of size-resolved carbonaceous material is the existence of positive and negative sampling artifacts related to the adsorption of volatile organic compounds (VOCs) and the adsorption or losses of semi-volatile organic compounds (SVOC). Positive artifacts were estimated by comparing TC measurements from the DLPI with those from several other systems used in this study (see Sect. 2.1 and Table 2). TC concentrations collected on all DLPI stages with $D_p < 2.5\ \mu\text{m}$ were summed (Fig. 4a). The regression for the entire dry season between the DLPI and the R2.5WW systems was: $TC_{(DLPI)} = 1.06 \cdot TC_{(R2.5WW)} + 4.4$, $r^2 = 0.89$; $n = 8$ (concentrations in $\mu\text{g m}^{-3}$; standard error of the slope: ± 0.36). This result indicates an overestimation for the impactor sampling (using only quartz fiber filters as substrates) that could be attributed to the positive artifact of VOCs and SVOCs. In comparison, the positive artifact averaged for the HVDS (UGent) was 5.2% (back filter to front filter OC concentration ratio of 0.052 ± 0.055).

TC concentrations were higher for the DLPI than the other samplers for the majority of day time samples (Fig. 4b and Table 2). A DLPI system with quartz fiber filters may overestimate between $\sim 15\%$ (night time) and $\sim 30\%$ (day time) of OC due to absorption of the SVOCs emitted during biomass burning. This behavior is expected, since during combustion events there are at least as much volatile organic gases emitted as aerosols (Robinson et al., 2007), and these gases might be collected by filter samplers, especially when using quartz fiber filters. Also, differences between day and night are expected because the gas-particle equilibrium moves towards the gas phase during the day due to the higher temperatures (Trebs et al., 2005).

Carbon content of aerosols from the burning of biomass

L. L. Soto-García et al.

Title Page

Abstract

Introduction

Conclusions

References

Tables

Figures

◀

▶

◀

▶

Back

Close

Full Screen / Esc

Printer-friendly Version

Interactive Discussion



Carbon content of aerosols from the burning of biomass

L. L. Soto-García et al.

[Title Page](#)[Abstract](#)[Introduction](#)[Conclusions](#)[References](#)[Tables](#)[Figures](#)[⏪](#)[⏩](#)[◀](#)[▶](#)[Back](#)[Close](#)[Full Screen / Esc](#)[Printer-friendly Version](#)[Interactive Discussion](#)

Another problem with cascade impactors is the determination of EC_a or BC_e , because deposits are usually not uniform on the sampling substrates. In Fig. 5 we compare the EC (EC_a and EC_w) and BC_e concentrations measured by different methods and techniques. The carbon monitor usually had concentrations more than three times higher than the other systems. With this system, EC_a was defined as the carbon content oxidized above 350°C (Artaxo et al., 2002), and most likely included significant amounts of OC. The EC_a measured with a thermal optical transmittance (TOT) system using both HVDS samplers from UGent was more than three times lower than the EC_w for all the other systems.

The TOT measurements are so much lower than those from all other techniques because the temperature program used in the TOT analysis (NIOSH standard temperature program) (Schmid et al., 2001) can affect the definition of the OC and EC split (Sciare et al., 2008; Chow et al., 2001, 2004; Schmid et al., 2001; Birch and Cary, 1996; NIOSH, 1996, 1999). Some additional insight comes from a comparison of the TOT(UGent) measurements with analyses of an additional sample set from LBA-SMOCC, where the TOT technique was used in parallel with the thermo-optical reflectance (TOR) technique (Chow et al., 2004). The data in Table 3 show that for the TC measurements, which are identical for the TOR and TOT techniques, there was good agreement between the two laboratories. However, the EC_a measurements by TOR are always much higher than those by TOT. This also applies to the TOT and TOR results by the Desert Research Institute (DRI) lab, where the TOR values are about a factor of two higher than the TOT values (excluding two outliers), even though they were obtained in the same runs and with the same temperature programs. The differences between the TOR and TOT results have been attributed to charring within the filter matrix, which leads to correction artefacts in TOT, but not in TOR (Chow et al., 2004). The even larger difference between the TOT values by UGent and the TOR measurements by DRI, which were on average 3.7 times higher, probably result from the use of a different instrument, different temperature calibration methods (Chow et al., 2005), and different temperature programs in addition to the TOR/TOT differences. Unfortunately,

the sample set analyzed at DRI did not overlap with the impactor sampling periods, making a direct comparison impossible.

The EC_w -HVDS (MPIC) measured using the EGA, after extraction with water, shows a high standard deviation which does not allow comparison with the other systems.

Results from the LTM, aethalometer (at two wavelengths, 571 nm and 880 nm), and TOA (after extracting with water and correcting for charring using 572 nm) were similar for BC_e and EC_w .

To help determine the source of the EC_a and BC_e , we plotted their concentrations as a function of TC concentrations for the fine fraction (sum of impactor stages with nominal $D_p < 2.5 \mu\text{m}$). Figure 6a and b shows a good correlation of EC_a , $EC_{a572 \text{ nm}}$, $EC_{w572 \text{ nm}}$ and BC_e with TC ($r^2 \sim 0.96, 0.99, 0.75$ and 0.81 , respectively), suggesting that carbonaceous aerosols were from biomass burning. This was expected for the dry season since there were many fires in the region (Fuzzi et al., 2007). The EC_a , EC_w , and BC_e /TC mass ratios per stage for each sample are given in Table 1.

The EC_a /TC slope in Fig. 6a shows an unrealistically high value of 0.51. This ratio is much higher than what has been previously reported for biomass burning samples in the same location (Mayol-Bracero et al., 2002a), and suggests that EC_a was strongly overestimated due to the presence of a large amount of refractory water-soluble material or OC char (Mayol-Bracero et al., 2002a; Hadley et al., 2008). Our results in Figure 6a and 6b for $EC_{a572 \text{ nm}}/TC$, $EC_{w572 \text{ nm}}/TC$, and BC_e/TC are 0.08, 0.07, and 0.04, respectively. These values are similar to those from a TOT method at the same site: 0.05 (Guyon et al., 2003); a two-step thermal analysis from Brazilian cerrado, grass, and forest fires: 0.08 (smoldering) (Ferek et al., 1998), and the values mentioned in the review by Reid et al. (2005), showing that smoke particles were 5–10% BC. Decesari et al. (2006) reported EC_w values of 7–19% of TC for the dry season during the SMOCC campaign. On the other hand, our EC_w were about three times higher than those measured by the UGent TOT analysis, suggesting that the latter represent an underestimation due to the use of the NIOSH protocol by the Gent group. Our values from the TOA and LTM methods indicated that 4–8% of the total carbon was atmospheric soot.

Carbon content of aerosols from the burning of biomass

L. L. Soto-García et al.

Title Page

Abstract

Introduction

Conclusions

References

Tables

Figures

⏪

⏩

◀

▶

Back

Close

Full Screen / Esc

Printer-friendly Version

Interactive Discussion



These results indicated that smoke particles were originating more from the smoldering phase of forest fires, as previously suggested by Mayol-Bracero et al. (2002a) and Reid et al. (2005).

In summary, our results show that all the methods used during LBA-SMOCC obtained reasonably comparable values for TC, with a modest overestimation in the impactor samples, probably due to the absorption of organic vapors (positive artefact). Large discrepancies were found between the various techniques used to determine EC_a and BC_e . In particular, the semi-continuous R&P Carbon Monitor gave excessively high values, probably due to a low OC/EC cutoff temperature that led to the inclusion of a significant amount of OC in the EC_a fraction. The EC_a analysis of the impactor samples without water extraction or optical correction also gave unrealistically high values. On the other hand, the TOT instrument using the NIOSH temperature program yielded very low values, possibly because of overcompensation of charring artefacts. The optical (BC_e) and the thermal methods with optical correction or water extraction gave mutually and internally consistent results with EC_a/TC or BC_e/TC ratios in the 0.04–0.08 range.

3.4 Absorption spectral dependence

The spectral dependence of the light attenuation was determined from the optical data obtained during thermal analysis (see Sect. 2.3.1). Figure 3b shows the spectral absorption of the smoke aerosol sample from Fig. 3a at 100 °C (see dashed line), before the evolution of any significant amount of carbon. The absorption Ångström exponent, α , was estimated by fitting a power law to the data: $\sigma(\lambda)=K\lambda^{-\alpha}$, where $\sigma(\lambda)$ is the spectrally dependent attenuation, K is a constant, λ is the light wavelength. The value of α is a measure of the strength of the spectral variation in aerosol light absorption. The absorption Ångström exponent was ~ 3.7 for our untreated and ~ 2.2 for our water-extracted biomass burning aerosol samples (Fig. 3b). In contrast, motor vehicle generated aerosols, in which the only light absorbing species is soot carbon, typically exhibit $\alpha \sim 1.0$ (Kirchstetter et al., 2004). The stronger spectral dependence of our

Carbon content of aerosols from the burning of biomass

L. L. Soto-García et al.

Title Page

Abstract

Introduction

Conclusions

References

Tables

Figures

◀

▶

◀

▶

Back

Close

Full Screen / Esc

Printer-friendly Version

Interactive Discussion



biomass smoke samples was due to the presence of light absorbing OC in addition to soot carbon (Schnaiter et al., 2003; Kirchstetter et al., 2004).

Water treatment removed much, but not all, of the sample OC that evolves below 400 °C (Fig. 3a). Similarly, the extraction with water greatly diminished the spectral dependence of the sample, but did not reduce all the samples to ~ 1.0 , as shown in Table 4. This table contains the absorption Ångström exponent results for the three samples that were measured by TOA (nominal D_p between 0.1–2.4 μm (stages 3–9)), the average was between 1.8 and 3.9 for the non-extracted samples, and between 0.7 and 1.6 for the extracted samples.

4 Contribution of the carbonaceous material to the total aerosol mass

Here we present an overview of the contribution of OC and BC_e (our approximation of soot carbon, C_{soot}) to the total aerosol mass. We chose BC_e concentrations determined by the LTM as the best representation of C_{soot} , since there were more samples analyzed by this method than by the other techniques. To estimate BC_e during the dry period for particles with $D_p < 2.5 \mu\text{m}$ we used DLPI stage 6 (nominal D_p in the range of 0.4–0.6 μm), where the concentration of BC_e was the highest and there was a good correlation between $\text{BC}_{e880 \text{ nm}}$ and TC. The regression line equation was $y = 0.02x + 0.51$; $r^2 = 0.86$.

Figure 7 presents a pie chart including the inorganic and carbonaceous components. For the carbonaceous fraction, the OC was estimated (TC- estimated BC_e) and converted to particle organic matter (POM) by using 1.8 as the conversion factor. This is a conservative OC conversion factor since aerosol heavily influenced by wood smoke can have conversion factors as high as 2.6 (Turpin and Lim, 2001). More than 85% of the total estimated mass was POM (Fig. 7). Our estimated OC concentration ($31.5 \mu\text{g m}^{-3}$) was similar to those reported by Decesari et al. (2006) for two HVDS sample sets from UGent (average: $31.6_{1\text{HVDS-UGent}} \mu\text{g m}^{-3}$ and $35.2_{2\text{HVDS-UGent}} \mu\text{g m}^{-3}$). Our OC concentrations averaged $44.0 \pm 18.3 \mu\text{g m}^{-3}$ (Table 1), accounting for $\sim 100\%$ of the car-

Carbon content of aerosols from the burning of biomass

L. L. Soto-García et al.

Title Page

Abstract

Introduction

Conclusions

References

Tables

Figures

◀

▶

◀

▶

Back

Close

Full Screen / Esc

Printer-friendly Version

Interactive Discussion



bonaceous aerosol in our samples. This result is not corrected for the positive artefact observed when using the DLPI (Fig. 4a).

These results indicate that, for biomass burning aerosols, using a thermal method only overestimates soot carbon and underestimates OC concentrations. Combining optical methods like LTM and TOA with solvent extraction may help in estimating the true atmospheric concentrations of C_{soot} and OC.

5 Size-resolved BC_e and POM

5.1 Size distribution biases

The DLPI size distributions measured using quartz fiber substrates have some biases, since for the standard DLPI impactors the aerodynamic diameter calculated for each stage is calibrated using smooth and flat surfaces, which are quite different from the surface characteristics of the quartz fiber filters. These introduce differences due to different flow rates and sampling mechanism (impaction together with filtration) (Hitzenberger et al., 2004; Saarikoski et al., 2008). Therefore, the D_p values and the shape of the collection efficiency curves may change, as has been shown by Saarikoski (2008). The carbonaceous size distributions presented in this study are expected to be shifted toward larger apparent diameters when using quartz filters (Saarikoski et al., 2008). More accurate DLPI size distributions could have been obtained by performing an inversion procedure (e.g., Bayesian inversion method (Ramachandran and Kandlikar, 1996), a bimodal lognormal function constructed by Dong et al. (2004), or a lognormal function for porous substrates suggested by Marjamäki et al., 2005), but the experimental data necessary to apply this procedure (i.e., calibration of impactor stage collection efficiencies, and the mathematical model function) are not available for the DLPI.

Figure 8 shows a comparison between TC concentrations collected with aluminum substrates and quartz fiber filters on the DLPI impactors. An exact comparison between the two DLPI substrates was not possible during this study, because sampling

Carbon content of aerosols from the burning of biomass

L. L. Soto-García et al.

Title Page

Abstract

Introduction

Conclusions

References

Tables

Figures

◀

▶

◀

▶

Back

Close

Full Screen / Esc

Printer-friendly Version

Interactive Discussion



of quartz and aluminum could not be done simultaneously. However, when all TC size distributions collected during the dry period on the aluminum substrates ($n = 7$) and the quartz fiber filters ($n = 13$) were compared, the TC concentrations for $D_p > \sim 0.4 \mu\text{m}$ (quartz fiber filters) were higher (by factors of 1.7–4.1) than the TC concentrations for the aluminum substrates. In other words, for aluminum TC is higher in fine diameters stages and lower on the coarse ones. Figure 8 shows that the size shift is less than one stage, i.e., significantly less than a factor of 2. Also, even though there is a shift in size when using quartz filters, the shape of the size distribution does not differ between the data sets from the two substrates.

5.2 Size distribution for POM and BC_e

The size distributions for the carbonaceous fraction (POM and BC_e) are presented in Fig. 9. Results show a bimodal distribution for BC_e , with a fine mode at D_p 0.4–0.6 μm and a small coarse mode at 6.7–10 μm . The BC_e coarse mode was probably due to an internal mixture of soot carbon and other coarse mode particles, or due to the absorption of light by large particles (e.g., primary biogenic aerosols) (Guyon et al., 2004). The size distributions in Fig. 9 clearly show a bimodal pattern for POM with peaks in the submicron (D_p 0.4–0.6 μm) and supermicron (D_p 2.4–4 μm) size range. The size distribution of BC_e was different from POM in the supermicron size, in part because the POM coarse mode may have been derived from plant debris, plant pollen and fungal spores. This has also been suggested by Fuzzi et al. (2007) for the size-resolved organic tracers of biogenic sources.

The similar shape of the profile of the accumulation mode for both POM and BC_e (Fig. 9) suggests that both species come from biomass burning. Previous studies have shown that the carbonaceous material (OC and EC) emitted from different sources showed an accumulation mode at 0.1 μm for EC and 0.1–0.3 μm for OC from diesel (Kerminen et al., 1997), 0.1–0.2 μm for POM and EC from cars (Kleeman et al., 2000), 0.2–0.3 μm volume size distribution from fresh biomass burning, and 0.3–0.4 μm volume size distribution from aged smoke (Reid et al., 2005). The submicron size range

Carbon content of aerosols from the burning of biomass

L. L. Soto-García et al.

Title Page

Abstract

Introduction

Conclusions

References

Tables

Figures

◀

▶

◀

▶

Back

Close

Full Screen / Esc

Printer-friendly Version

Interactive Discussion



we are reporting here is normally called the droplet mode (0.4–0.6 μm) and it is expected to occur with aged air masses due to cloud processing. Figure 10a demonstrates that POM mass concentrations were higher during the night. This increase in the fine fraction during night was mainly due to continued emissions into the shallow nocturnal boundary layer (Rissler et al., 2006), to the condensation of volatile compounds into the aerosol phase at the lower temperatures ($<25^\circ\text{C}$), and to high nocturnal relative humidity ($\sim 100\%$) (Trebs et al., 2005). OC enrichment was also observed in the size-resolved low molecular weight WSOC fractions measured by Falkovich et al. (2005) and Fuzzi et al. (2007). However, Fig. 10b shows that the fine mode mass of BC_e during day time was almost the same as during night time, suggesting that little additional soot carbon is emitted at night. This supported the findings of Hoffer et al. (2006b) that during the day flaming, which produces more atmospheric soot (Reid et al., 2005; Simoneit, 2002), was the dominant combustion phase and that smoldering dominated during the night. The size distributions of both POM and BC_e are shifted slightly towards larger sizes at night, possibly due to some condensation of organic and inorganic constituents, as well as some water uptake.

6 Conclusions

In this study, as part of the SMOCC-2002 field experiment, we compared analyses with different techniques of the carbonaceous fraction in aerosol samples dominated by biomass burning. Results from thermal, thermal-optical (TOA) and optical techniques applied to water-extracted and non-extracted samples showed that most of the aerosol mass was due to carbonaceous material, and that the fine fraction was greater than the coarse fraction. TOA showed that the WSOC fraction was at least partly pyrolyzed during the analysis. Also, for specific sizes (D_p : 0.2–0.3 and 0.4–0.6 μm), TOA showed the existence of residual OC on water extracted samples. This contradicts the assumption sometimes made for analysis of aerosols from biomass burning sources, that only EC remains after water extraction.

Carbon content of aerosols from the burning of biomass

L. L. Soto-García et al.

Title Page

Abstract

Introduction

Conclusions

References

Tables

Figures



Back

Close

Full Screen / Esc

Printer-friendly Version

Interactive Discussion



Carbon content of aerosols from the burning of biomass

L. L. Soto-García et al.

[Title Page](#)[Abstract](#)[Introduction](#)[Conclusions](#)[References](#)[Tables](#)[Figures](#)[◀](#)[▶](#)[◀](#)[▶](#)[Back](#)[Close](#)[Full Screen / Esc](#)[Printer-friendly Version](#)[Interactive Discussion](#)

Different techniques commonly used for determining EC_a produced different results, demonstrating the difficulties of separating EC from OC in biomass burning samples. Burning of biomass produces EC_a and OC with similar thermal, oxidative and optical characteristics. Based on our results, we suggest the aethalometer, LTM, TOR, and TOA together with solvent extraction methods as the most suitable techniques for the estimation of atmospheric soot carbon.

Different temperature programs showed significant differences. For example, measurements with the semi-continuous R&P carbon monitor yielded EC_a concentrations that were more than three times higher than for most other systems. In contrast, the TOT method gave EC_a concentrations that were more than three times lower than most other systems. EC_a and BC_e contributed 4 to 8% to the total mass concentration. The POM contribution was more than 85%.

TC and POM mass-size distributions were bimodal with the submicron fraction significantly larger than the coarse fraction. BC_e showed the expected mode in the submicron size and a mode in the coarse size, possibly due to an internal mixture of BC_e and other coarse particles, that require further study. Diurnal variations of OC were also observed. The different diurnal behavior of the OC and BC_e size distributions supports the prevalence of different combustion phases during daytime (mostly flaming) and nighttime (mostly smoldering).

We conclude that LTM, TOR, and TOA together with water-extraction provided the best estimates of EC_a and BC_e concentrations and size distributions of aerosols dominated by biomass burning. The use of these techniques can reduce the uncertainties in the estimation of EC_a or BC_e , and, therefore, provide more reliable data to be used by global and regional climate models that deal with the impact of biomass burning.

Acknowledgements. This work was carried out within the framework of the *Smoke, Aerosols, Clouds, Rainfall, and Climate* (SMOCC) project, a European contribution to the Large-Scale Biosphere-Atmosphere Experiment in Amazonia (LBA). It was financially supported by the NASA-Puerto Rico Space Grant Consortium and the Max Planck Society (MPG). Willy Maenhaut also thanks the Belgian Federal Science Policy Office for research support. We are thank-

ful to all members of the LBA-SMOCC team, to Susimar González for her help in the collection of samples, and to Pascal Guyon for some of the thermal analyses.

References

- 5 Andreae, M. O., Artaxo, P., Brandão, C., Carswell, F. E., Ciccioli, P., da Costa, A. L., Culf, A. D., Esteves, J. L., Gash, J. H. C., Grace, J., Kabat, P., Lelieveld, J., Malhi, Y., Manzi, A. O., Meixner, F. X., Nobre, A. D., Nobre, C., Ruivo, M. D. L. P., Silva-Dias, M. A., Stefani, P., Valentini, R., von Jouanne, J., and Waterloo, M. J.: Biogeochemical cycling of carbon, water, energy, trace gases and aerosols in Amazonia: The LBA-EUSTACH experiments, *J. Geophys. Res.*, 107, 8066, doi:10.1029/2001JD000524, 2002.
- 10 Andreae, M. O. and Crutzen, P.: Atmospheric Aerosols: Biogeochemical Sources and Role in the Atmospheric Chemistry, *Science*, 276, 1052–1058, 1997.
- Andreae, M. O. and Gelencsér, A.: Black carbon or brown carbon? The nature of light-absorbing carbonaceous aerosols, *Atmos. Chem. Phys.*, 6, 3131–3148, doi:10.5194/acp-6-3131-2006, 2006.
- 15 Andreae, M. O., Rosenfeld, D., Artaxo, P., Costa, A. A., Frank, G. P., Longo, K. M., and Silva-Dias, M. A. F.: Smoking rain clouds over the Amazon, *Science*, 303, 1337–1342, 2004.
- Artaxo, P., Fernandez, E. T., Martins, J. V., Yamasoe, M. A., Hobbs, P. V., Maenhaut, W., Longo, K. M., and Castanho, A.: Large scale aerosol source apportionment in Amazonia, *J. Geophys. Res.*, 103, 31837–31848, 1998.
- 20 Artaxo, P., de Campos, R. C., Fernandez, E. T., Martins, J. V., Xiao, Z., Lindqvist, O., Fernandez-Jimenez, M. T., and Maenhaut, W.: Large scale mercury and trace element measurements in the Amazon Basin, *Atmos. Environ.*, 34, 4085–4096, 2000.
- Artaxo, P., Vanderlei Martins, J., Yamasoe, M. A., Procopio, A. S., Pauliquevis, T. M., Andreae, M. O., Guyon, P., Gatti, L. V., and Cordova Leal, A. M.: Physical and chemical properties of aerosols in the wet and dry seasons in the Rondônia, Amazonia, *J. Geophys. Res.*, 25 107(D20), 8066, doi:10.1029/2001JD000666, 2002.
- Barth, M., Mc Fadden, J., Sun, J., Wiedinmyer, C., Chuang, P., Collins, D., Griffin, R., Hannigan, M., Karl, T., Kim, S., Lasher-Trapp, S., Levis, S., Litvak, M., Mahowald, N., Moore, K., Nandi, S., Nemitz, E., Nenes, A., Potosnak, M., Raymond, T., Smith, J., Still, C., and Stroud, C.:

Carbon content of aerosols from the burning of biomass

L. L. Soto-García et al.

Title Page

Abstract

Introduction

Conclusions

References

Tables

Figures

◀

▶

◀

▶

Back

Close

Full Screen / Esc

Printer-friendly Version

Interactive Discussion



Carbon content of aerosols from the burning of biomass

L. L. Soto-García et al.

Title Page

Abstract

Introduction

Conclusions

References

Tables

Figures

◀

▶

◀

▶

Back

Close

Full Screen / Esc

Printer-friendly Version

Interactive Discussion



Coupling between land ecosystems and the atmospheric hydrologic cycle through biogenic aerosol pathways, *B. Am. Meteorol. Soc.*, 1738–1742, 2005.

Birch, M. E. and Cary, R. A.: Elemental carbon-based method for monitoring occupational exposures to particulate diesel exhaust, *Aerosol. Sci. Technol.*, 25, 221–241, 1996.

5 Chen, L.-W. A., Chow, J. C., Watson, J. G., Moosmiller, H., Arnott, P. W.: Modeling reflectance and transmittance of quartz-fiber filter samples containing elemental carbon particles: Implication for thermal/optical analysis, *J. Aerosol Sci.*, 35, 765–780, 2004.

Chow, J. C., Watson, J. G., Pritchett, L. C., Pierson, W. R., Frazier, C. A., and Purcell, R. G.: The DRI Thermal/Optical Reflectance carbon analysis system: Description, evaluation and applications in U.S. air quality studies, *Atmos. Environ.*, 27A, 8, 1185–1201, 1993.

10 Chow, J. C., Watson, J. G., Crow, D., Lowenthal, D. H., and Merrifield, T.: Comparison of IMPROVE and NIOSH carbon measurements, *Aerosol. Sci. Technol.*, 34, 23–34, 2001.

Chow, J. C., Watson, J. G., Chen, L. W. A., Arnott, W. P., and Moosmüller, H., Equivalence of elemental carbon by thermal/optical reflectance and transmittance with different temperature protocols, *Environ. Sci. Technol.*, 38, 4414–4422, 2004.

15 Chow, J. C., Watson, J. G., Chen, L.-W. A., Paredes-Miranda, G., Chang, M.-C. O., Trimble, D., Fung, K. K., Zhang, H., and Zhen Yu, J.: Refining temperature measures in thermal/optical carbon analysis, *Atmos. Chem. Phys.*, 5, 2961–2972, doi:10.5194/acp-5-2961-2005, 2005.

20 Chow, J. C., Watson, J. G., Chen, L.-W. A., Chang, M. C. O., Robinson, N. F., Trimble, D., and Kohl, S. D.: The IMPROVE.A temperature protocol for thermal/optical carbon analysis: Maintaining consistency with a long-term database, *J. Air Waste Manage. Assoc.*, 57(9), 1014–1023, 2007.

25 Decesari, S., Fuzzi, S., Facchini, M. C., Mircea, M., Emblico, L., Cavalli, F., Maenhaut, W., Chi, X., Schkolnik, G., Falkovich, A., Rudich, Y., Claeys, M., Pashynska, V., Vas, G., Kourtchev, I., Vermeylen, R., Hoffer, A., Andreae, M. O., Tagliavini, E., Moretti, F., and Artaxo, P.: Characterization of the organic composition of aerosols from Rondônia, Brazil, during the LBA-SMOCC 2002 experiment and its representation through model compounds, *Atmos. Chem. Phys.*, 6, 375–402, doi:10.5194/acp-6-375-2006, 2006.

Dod, R. L., Rosen, H., and Novakov T.: Optico-thermal analysis of the carbonaceous fraction of aerosol particles, Rep. LBL-8696, Lawrence Berkeley Lab., Berkeley, Calif., 1979.

30 Dong, Y., Hays, M. D., Smith, N. D., and Kinsey, J. S.: Inverting cascade impactor data for size-resolved characterization of fine particulate source emissions, *J. Aerosol Sci.*, 35, 1497–1512, 2004.

Carbon content of aerosols from the burning of biomass

L. L. Soto-García et al.

Title Page

Abstract

Introduction

Conclusions

References

Tables

Figures

◀

▶

◀

▶

Back

Close

Full Screen / Esc

Printer-friendly Version

Interactive Discussion



EPA (US Environmental Protection Agency) Publication: Particle pollution and your health, 452/F-03-001, available at: <http://www.epa.gov/airnow//particle/pm-color.pdf>, (last access: June 2008), 2003.

5 Falkovich, A. H., Graber, E. R., Schkolnik, G., Rudich, Y., Maenhaut, W., and Artaxo, P.: Low molecular weight organic acids in aerosol particles from Rondônia, Brazil, during the biomass-burning, transition and wet periods, *Atmos. Chem. Phys.*, 5, 781–797, doi:10.5194/acp-5-781-2005, 2005.

Ferek, R. J., Reid, J. S., Hobbs, P. V., Blake, D. R., and Liousse, C.: Emission factors of hydrocarbons, halocarbons, trace gases and particles from biomass burning in Brazil, *J. Geophys. Res.*, 103, 32107–32118, 1998.

10 Formenti, P., Elbert, W., Maenhaut, W., Haywood, J., Osborne, S., and Andreae, M. O.: Inorganic and carbonaceous aerosols during the Southern African Regional Science Initiative (SAFARI 2000) experiment: Chemical characteristics, physical properties, and emission data for smoke from African biomass burning, *J. Geophys. Res.*, 108(D13), 8488, doi:10.1029/2002JD002408, 2003.

15 Fuzzi, S., Decesari, S., Facchini, M. C., Cavalli, F., Emblico, L., Mircea, M., Andreae, M. O., Trebs, I., Hoffer, A., Guyon, P., Artaxo, P., Rizzo, L. V., Lara, L. L., Pauliquevis, T., Maenhaut, W., Raes, N., Chi, X., Mayol-Bracero, O. L., Soto-García, L. L., Claeys, M., Kourtchev, I., Rissler, J., Swietlicki, E., Tagliavini, E., Schkolnik, G., Falkovich, A. H., Rudich, Y., Fisch, G., and Gatti, L. V.: Overview of the inorganic and organic composition of size-segregated aerosol in Rondônia, Brazil, from the biomass-burning period to the onset of the wet season, *J. Geophys. Res.*, 112, D01201, doi:10.1029/2005JD006741, 2007.

20 Graham, B., Mayol-Bracero, O. L., Guyon, P., Roberts, G. C., Decesari, S., Facchini, M. C., Artaxo, P., Maenhaut, W., Köll, P., and Andreae, M. O.: Water-soluble organic compounds in biomass burning aerosols over Amazonia, 1. Characterization by NMR and GC-MS, *J. Geophys. Res.*, 107(D20), 8047, doi:10.1029/2001JD000336, 2002.

Gundel, L. A., Dod, R. L., Rosen, H., and Novakov, T.: The relationship between optical attenuation and black carbon concentrations for ambient and source particles, *Sci. Total Environ.*, 36, 197–202, 1984.

30 Guyon, P., Graham, B., Roberts, G., Mayol-Bracero, O., Maenhaut, W., Artaxo, P., and Andreae, M.: In-canopy gradients, composition, sources, and optical properties of aerosol over the Amazon forest, *J. Geophys. Res.*, 108(D18), 4591, doi:10.1029/2003JD003465, 2003.

Guyon, P., Graham, B., Roberts, G. C., Mayol-Bracero, O. L., Maenhaut, W., Artaxo, P., and

Carbon content of aerosols from the burning of biomass

L. L. Soto-García et al.

[Title Page](#)[Abstract](#)[Introduction](#)[Conclusions](#)[References](#)[Tables](#)[Figures](#)[◀](#)[▶](#)[◀](#)[▶](#)[Back](#)[Close](#)[Full Screen / Esc](#)[Printer-friendly Version](#)[Interactive Discussion](#)

Andreae, M. O.: Sources of optically active aerosol particles over the Amazon forest, *Atmos. Environ.*, 38, 1039–1051, 2004.

Hadley, O, Corrigan, C., and Kirchstetter, T.: Modified thermal-optical analysis using spectral absorption selectivity to distinguish black carbon from pyrolyzed organic carbon, *Environ. Sci. Technol.*, 42, 8459–8464, 2008.

Hansen, A. D. A., Rosen, H., and Novakov, T.: The aethalometer—an instrument for the real-time measurement of optical absorption by aerosol particles, *Sci. Total Environ.*, 36, 91–196, 1984.

Herckes, P., Eregling, G., Kreidenweis, S., and Collett, J.: Particle size distributions of organic aerosol constituents during the 2002 Yosemite aerosol characterization study, *Environ. Sci. Technol.*, 40, 4554–4562, 2006.

Hitzenberger, R., Berner, A., Galambos, Z., Maenhaut, W., Cafmeyer, J., Schwarz, J., Müller, K., Spindler, G., Wiedprecht, W., Acker, K., Hillamo, R., and Mäkelä, T.: Intercomparison of methods to measure the mass concentration of the atmospheric aerosol during INTERCOMP2000—influence of instrumentation and size cuts, *Atmos. Environ.*, 38, 6467–6476, 2004.

Hobbs, P. V., Reid, J. S., Kotchenruther, R. A., Ferek, R. J., and Weiss, R.: Direct radiative forcing by smoke from biomass burning, *Science*, 272, 1776–1778, 1997.

Hoffer, A., Gelencsér, A., Guyon, P., Kiss, G., Schmid, O., Frank, G. P., Artaxo, P., and Andreae, M. O.: Optical properties of humic-like substances (HULIS) in biomass-burning aerosols, *Atmos. Chem. Phys.*, 6, 3563–3570, doi:10.5194/acp-6-3563-2006, 2006a.

Hoffer, A., Gelencsér, A., Blazsó, M., Guyon, P., Artaxo, P., and Andreae, M. O.: Diel and seasonal variations in the chemical composition of biomass burning aerosol, *Atmos. Chem. Phys.*, 6, 3505–3515, doi:10.5194/acp-6-3505-2006, 2006b.

Kerminen, V.-M., Makela, T. E., Ojanen, C. H., Hillamo, R. E., Vilhunen, J. K., Rantanen, L., Havers, N., Von Bohlen, A., and Klockow, D.: Characterisation of the particulate phase in the exhaust of a diesel car, *Environ. Sci. Technol.*, 31, 1883–1889, 1997.

Kleeman, M. J., Schauer, J. J., and Cass, G. R.: Size and composition distribution of fine particulate matter emitted from motor vehicles, *Environ. Sci. Technol.*, 34, 1132–1142, 2000.

Kirchstetter, T. W., Corrigan, C. E., and Novakov, T.: Laboratory and field investigation of the adsorption of gaseous organic compounds onto quartz filters, *Atmos. Environ.*, 35, 1663–1671, 2001.

Kirchstetter, T. W., Novakov, T., Hobbs, P. V., and Magi, B.: Airborne measurements of carbona-

Carbon content of aerosols from the burning of biomass

L. L. Soto-García et al.

[Title Page](#)[Abstract](#)[Introduction](#)[Conclusions](#)[References](#)[Tables](#)[Figures](#)[◀](#)[▶](#)[◀](#)[▶](#)[Back](#)[Close](#)[Full Screen / Esc](#)[Printer-friendly Version](#)[Interactive Discussion](#)

ceous aerosols in southern Africa during the dry, biomass burning season, *J. Geophys. Res.*, 108(D13), 8476, doi:10.1029/2002JD002171, 2003.

Kirchstetter, T. W., Novakov, T., and Hobbs, P. V.: Evidence that the spectral dependence of light absorption by aerosols is affected by organic carbon, *J. Geophys. Res.*, 109, D21208, doi:10.1029/2004JD0004999, 2004.

Kirchstetter, T. W. and Novakov, T.: Controlled generation of black carbon particles from a diffusion flame and applications in evaluating black carbon measurement methods, *Atmos. Environ.*, 41, 1874–1888, 2007.

Kirkman, G. A., Gut, A., Ammann, C., Gatti, L. V., Cordova, A. M., Moura, M. A. L., Andreae, M. O., and Meixner, F. X.: Surface exchange of nitric oxide, nitrogen dioxide, and ozone at a cattle pasture in Rondonia, Brazil, *J. Geophys. Res.*, 107(D20), 8083, doi:10.1029/2001JD000523, 2002.

Koren, I., Kaufman, Y. J., Remer, L. A., and Martins, J. V.: Measurement of the effect of Amazon smoke on inhibition of cloud formation, *Science*, 303, 1342–1345, 2004.

Marjamäki, M., Lemmetty, M., and Keskinen, J.: ELPI response and data reduction I: response function, *Aerosol. Sci. Technol.*, 39, 575–582, 2005.

Martins, J. V., Artaxo, P., Lioussé, C., Reid, J. S., Hobbs, P. V., and Kaufman, Y. J.: Effects of black carbon content, particle size, and mixing on light absorption by aerosols from biomass burning in Brazil, *J. Geophys. Res.*, 103, 32041–32050, 1998a.

Martins, J. V., Hobbs, P. V., Weiss, R. E., and Artaxo, P.: Sphericity and morphology of smoke particles from biomass burning in Brazil, *J. Geophys. Res.*, 103, 32051–32057, 1998b.

Mayol-Bracero, O. L., Guyon, P., Graham, B., Andreae, M. O., Decesari, S., Facchini, M. C., Fuzzi, S., and Artaxo, P.: Water-soluble organic compounds in biomass burning aerosols over Amazonia, 2. Apportionment of the chemical composition and importance of the polyacidic fraction, *J. Geophys. Res.*, 107(D20), 8091, doi:10.1029/2001JD000522, 2002a.

Mayol-Bracero, O. L., Gabriel, R., Andreae, M. O., Kirchstetter, T. W., Novakov, T., and Streets, D. G.: Carbonaceous aerosols over the Indian Ocean during INDOEX: Chemical characterization, optical properties, and probable sources, *J. Geophys. Res.*, 107(D19), 8030, doi:10.1029/2000JD000039, 2002b.

Mircea, M., Facchini, M. C., Decesari, S., Cavalli, F., Emblico, L., Fuzzi, S., Vestin, A., Rissler, J., Swietlicki, E., Frank, G., Andreae, M. O., Maenhaut, W., Rudich, Y., and Artaxo, P.: Importance of the organic aerosol fraction for modeling aerosol hygroscopic growth and activation: a case study in the Amazon Basin, *Atmos. Chem. Phys.*, 5, 3111–3126, doi:10.5194/acp-5-

Carbon content of aerosols from the burning of biomass

L. L. Soto-García et al.

Title Page

Abstract

Introduction

Conclusions

References

Tables

Figures

◀

▶

◀

▶

Back

Close

Full Screen / Esc

Printer-friendly Version

Interactive Discussion



3111-2005, 2005.

NIOSH: Elemental carbon (diesel exhaust), in: NIOSH manual of analytical methods, National Institute of Occupational Safety and Health, Cincinnati, OH, 1996.

NIOSH: Method 5040 issue 3 (interim): elemental carbon (diesel exhaust), in: NIOSH manual of analytical methods, National Institute of Occupational Safety and Health, Cincinnati, OH, 1999.

Novakov, T.: Microchemical characterization of aerosols, in: Nature, Aim and Methods of Microchemistry, edited by: Malissa, H., Grasserbaure, M., and Belcher, R., Springer-Verlag, New York, 141–165, 1981.

Novakov, T. and Corrigan, C. E.: Thermal characterization of biomass smoke particles, *Mikrochim. Acta*, 119, 157–166, 1995.

Park, K., Chow, J. C., Watson, J. G., Trimble, D. L., Doraiswamy, P., Arnott, W. P., Stroud, K. R., Bowers, K., Bode, R., Petzold, A., and Hansen, A. D. A.: Comparison of continuous and filter-based carbon measurements at the Fresno Supersite, *J. Air Waste Manage. Assoc.*, 56(4), 474–491, 2006.

Peterson, M. R. and Richards, M. H.: Thermal-optical transmittance analysis for organic, elemental, carbonate, total carbon, and OCX2 in PM_{2.5} by the EPA/NIOSH method, in: Proceedings, Symposium on Air Quality Measurement Methods and Technology-2002, edited by: Winegar, E. D. and Tropp, R. J., *J. Air Waste Manage. Assoc.*, Pittsburgh, PA, 83-1–83-19, 2002.

Pope, C. A. and Dockery, D. W.: Health effects of fine particulate air pollution: Lines that connect, *J. Air Waste Manage. Assoc.*, 56, 709–742, 2006.

Pöschl, U.: Aerosol particle analysis: challenges and progress, *Anal. Bioanal. Chem.*, 375, 30–32, 2003.

Ramachandran, G. and Kandlikar, M.: Bayesian analysis for the inversion of aerosols from impaction data, *J. Aerosol Sci.*, 27, 1099–1112, 1996.

Reid, J. S., Hobbs, P. V., Ferek, R. J., Blake, D. R., Martins, J. V., Dunlap, M. R., and Liousse, C.: Physical, chemical, and optical properties of regional hazes dominated by smoke in Brazil, *J. Geophys. Res.*, 103, 32059–32080, 1998.

Reid, J. S., Koppmann, R., Eck, T. F., and Eleuterio, D. P.: A review of biomass burning emissions part II: intensive physical properties of biomass burning particles, *Atmos. Chem. Phys.*, 5, 799–825, doi:10.5194/acp-5-799-2005, 2005.

Rissler, J., Vestin, A., Swietlicki, E., Fisch, G., Zhou, J., Artaxo, P., and Andreae, M. O.: Size

Carbon content of aerosols from the burning of biomass

L. L. Soto-García et al.

[Title Page](#)[Abstract](#)[Introduction](#)[Conclusions](#)[References](#)[Tables](#)[Figures](#)[◀](#)[▶](#)[◀](#)[▶](#)[Back](#)[Close](#)[Full Screen / Esc](#)[Printer-friendly Version](#)[Interactive Discussion](#)

distribution and hygroscopic properties of aerosol particles from dry-season biomass burning in Amazonia, *Atmos. Chem. Phys.*, 6, 471–491, doi:10.5194/acp-6-471-2006, 2006.

Robinson, A. L., Donahue, N. M., Shrivastava, M. K., Weikamp, E. A., Sage, A. M., Grieshop, A. P., Lane, T. E., Pierce, J. R., and Pandis, S. N.: Rethinking organic aerosols: semivolatile emissions and photochemical aging, *Science*, 315, 1259–1262, 2007.

Rosenfeld, D.: TRMM Observed first direct evidence of smoke from forest fires inhibiting rainfall, *Geophys. Res. Lett.*, 26, 3105–3108, 1999.

Rosenfeld, D., Lohmann, U., Raga, G. B., O'Dowd, C. D., Kulmala, M., Fuzzi, S., and Reissell, A.: Flood or drought: How do aerosols affect precipitation?, *Science*, 321, 1309–1313, 2008.

Salmon, L. G., Hildemann, L. M., Mazurek, M., Christoforou, C., Frei, N. A., Solomon, P. A., Schauer, J., Hughes, L., and Johnson, R.: Procedures Manual, Environ. Qual. Laboratory, Calif. Inst. of Technol., Pasadena, Calif., August 1998.

Saarikoski, S., Frey, A., Mäkelä, T., and Hillamo, R.: Size distribution measurement of carbonaceous particulate matter using a low pressure impactor with quartz fiber substrates, *Aerosol. Sci. Technol.*, 42, 603–612, 2008.

Schmid, H., Laskus, L., Abraham, H. J., Baltensperger, U., Lavanchy, V., Bizjak, M., Burba, P., Cachier, H., Crow, D., Chow, J., Gnauk, T., Even, A., ten Brink, H. M., Giesen, K.-P., Hitenberger, R., Hueglin, C., Maenhaut, W., Pio, C., Carvalho, A., Putaud, J.-P., Toom-Saunty, D., and Puxbaum, H.: Results of the carbon conference international aerosol carbon round robin test stage I, *Atmos. Environ.*, 35, 2111–2121, 2001.

Schmid, O., Artaxo, P., Arnott, W. P., Chand, D., Gatti, L. V., Frank, G. P., Hoffer, A., Schnaiter, M., and Andreae, M. O.: Spectral light absorption by ambient aerosols influenced by biomass burning in the Amazon Basin. I: Comparison and field calibration of absorption measurement techniques, *Atmos. Chem. Phys.*, 6, 3443–3462, doi:10.5194/acp-6-3443-2006, 2006.

Schnaiter, M., Horvath, H., Mohler, O., Naumann, K. H., Saathoff, H., and Schock, O. W.: UV-VIS-NIR spectral optical properties of soot and soot-containing aerosols, *J. Aerosol Sci.*, 34, 1421–1444, 2003.

Sciare, J., Oikonomou, K., Favez, O., Liakakou, E., Markaki, Z., Cachier, H., and Mihalopoulos, N.: Long-term measurements of carbonaceous aerosols in the Eastern Mediterranean: evidence of long-range transport of biomass burning, *Atmos. Chem. Phys.*, 8, 5551–5563, doi:10.5194/acp-8-5551-2008, 2008.

Simoneit, B. R. T.: Biomass burning – A review of organic tracers for smoke from incomplete combustion, *Appl. Geochem.*, 17, 129–162, 2002.

Carbon content of aerosols from the burning of biomass

L. L. Soto-García et al.

Title Page

Abstract

Introduction

Conclusions

References

Tables

Figures

⏪

⏩

◀

▶

Back

Close

Full Screen / Esc

Printer-friendly Version

Interactive Discussion



Solomon, P. A., Moyers, J. L., and Fletcher, R. A.: High-volume dichotomous virtual impactor for the fractionation and collection of particles according to aerodynamic size, *Aerosol Sci. Technol.*, 2, 455–464, 1983.

5 Trebs, I., Metzger, S., Meixner, F. X., Helas, G., Hoffer, A., Rudich, Y., Falkovich, A., Moura, M. A. L., Da Silva, R. J., Artaxo, P., Slanina, J., and Andreae, M. O.: The NH_4^+ - NO_3^- - Cl^- - SO_4^{2-} - H_2O aerosol system and its gas phase precursors at a pasture site in the Amazon Basin: How relevant are mineral cations and soluble organic acids?, *J. Geophys. Res.*, 110, D07303, doi:10.1029/2004JD005478, 2005.

10 Turpin, B. and Lim, H.: Species contributions to $\text{PM}_{2.5}$ mass concentrations: revisiting common assumption for estimating organic mass, *Aerosol. Sci. Technol.*, 35, 602–610, 2001.

Watson, J. G., Chow, J. C., and Chen, L.-W. A.: Summary of organic and elemental carbon/black carbon analysis methods and intercomparisons, *Aerosol Air Qual. Res.*, 5(1), 65–102, 2005.

15 Watson, J. G., Chow, J. C., and Chen, L.-W. A.: Methods to assess carbonaceous aerosol sampling artifacts for IMPROVE and other long-term networks, *J. Air Waste Manage. Assoc.*, 59(8), 898–911, 2009.

Zhen, J., Xu, J., and Yang, H.: Charring characteristics of atmospheric organic particulate matter in thermal analysis, *Environ. Sci. Technol.*, 36, 754–761, 2002.

Carbon content of aerosols from the burning of biomass

L. L. Soto-García et al.

Table 1. Concentration of the size-resolved carbonaceous component collected at the pasture site (FNS) during the dry period for the LBA-SMOCC campaign using different methods (EGA, LTM and Aethalometer). All concentrations are given in $\mu\text{g m}^{-3}$. nm indicates not measured. The last two columns are for the equivalent black carbon (BC_e) at two wavelengths for particles with $D_p < 10 \mu\text{m}$.

DLPI #	Date	Method used =>		TC	EC_a	EC_a /TC	EGA*				$\text{EC}_{\text{w}572 \text{ nm}}$ (extracted)	$\text{EC}_{\text{w}572 \text{ nm}}$ (extracted)/ TC	BC_e 880 nm	LTM** $\text{BC}_{\text{e}880 \text{ nm}}/$ TC	OC	Aethalometer					
		Volume (m^3)	Size Cut (μm)				EC_a 572 nm (non- extracted)	EC_a 572 nm (non- extracted)/TC	EC_a 572 nm (non- extracted)/TC	EC_a 572 nm (non- extracted)/TC						BC_e 571 nm	BC_e 880 nm				
3	17 Sep – night	21.4	0.070	0.075	0.42	0.13	0.31	NM	NM	NM	NM	0.05	0.12	0.37	5.43	6.06					
			0.075	0.103	0.61	0.22	0.36	NM	NM	NM	NM	0.06	0.10	0.55							
			0.103	0.162	1.64	0.74	0.45	NM	NM	NM	NM	0.13	0.08	1.51							
			0.162	0.269	4.75	2.11	0.44	NM	NM	NM	NM	0.29	0.06	4.46							
			0.269	0.392	9.2	4.15	0.45	NM	NM	NM	NM	0.52	0.06	8.67							
			0.392	0.627	19.47	9.92	0.51	NM	NM	NM	NM	0.84	0.04	18.63							
			0.627	0.968	14.09	6.00	0.43	NM	NM	NM	NM	0.7	0.05	13.39							
			0.968	1.632	8.83	3.20	0.36	NM	NM	NM	NM	0.68	0.08	8.15							
			1.632	2.439	3.4	1.25	0.37	NM	NM	NM	NM	0.48	0.14	2.92							
			2.439	4.081	2.72	0.84	0.31	NM	NM	NM	NM	0.3	0.11	2.42							
			4.081	6.721	1.85	0.54	0.29	NM	NM	NM	NM	0.13	0.07	1.72							
			6.721	10.157	0.97	0.31	0.32	NM	NM	NM	NM	0.19	0.20	0.78							
			10.157	30	0.96	0.27	0.28	NM	NM	NM	NM	0.09	0.09	0.86							
			Fine	62.41	27.72	0.44	NM	NM	NM	NM	NM	3.75	0.06	58.65							
			Coarse	6.50	1.96	0.30	NM	NM	NM	NM	NM	0.71	0.11	5.78							
			11	26 Sep – day	12.6	0.054	0.067	0.61	0.16	0.27	0.13	0.21	0.05	0.08			0.11	0.18	0.5	2.58	3.03
						0.067	0.100	0.84	0.29	0.35	0.2	0.24	0.02	0.02			0.02	0.02	0.82		
0.100	0.160	2.66				1.00	0.37	0.46	0.17	0.25	0.09	0.12	0.05	2.54							
0.160	0.268	6.88				2.66	0.39	0.61	0.09	0.56	0.08	0.43	0.06	6.44							
0.268	0.390	12.55				4.68	0.37	1.34	0.11	0.6	0.05	0.56	0.04	11.99							
0.390	0.625	16.77				5.54	0.33	1.77	0.11	1.53	0.09	0.88	0.05	15.89							
0.625	0.965	9.83				3.53	0.36	1.15	0.12	0.89	0.09	0.63	0.06	9.2							
0.965	1.627	3.29				1.39	0.42	0.59	0.18	0.28	0.09	0.25	0.08	3.03							
1.627	2.430	1.49				0.60	0.40	0.4	0.27	0.07	0.05	0	0.00	1.49							
2.430	4.067	0.98				0.27	0.27	0.27	0.28	0.03	0.03	0.08	0.08	0.89							
4.067	6.698	0.1				0.05	0.49	-	-	0.04	0.40	0.09	0.90	0.01							
6.698	10.122	-				0.04	-	-	-	-	0.02	-	-	-							
10.122	30.0	0.65				0.33	0.51	-	-	-	0	0.00	0.65	-							
Fine	54.92	19.86				0.36	6.65	0.12	4.25	0.08	3.00	0.05	51.90	-							
Coarse	1.73	0.69				0.40	0.27	0.16	0.07	0.04	0.19	0.11	1.55	-							

Title Page

Abstract

Introduction

Conclusions

References

Tables

Figures

◀

▶

◀

▶

Back

Close

Full Screen / Esc

Printer-friendly Version

Interactive Discussion



Carbon content of aerosols from the burning of biomass

L. L. Soto-García et al.

Table 1. Continued.

DLPI #	Date	Method used =>		TC	EC _a	EC _a /TC	EGA*		EC _{w572 nm} (extracted)	EC _{w572 nm} (non-extracted)/TC	BC _e 880 nm	LTM**		OC	Aethalometer	
		Volume (m ³)	Size Cut (µm)				EC _a 572 nm (non-extracted)	EC _a 572 nm (non-extracted)/TC				BC _e 880 nm/TC	BC _e 571 nm		BC _e 880 nm	
12	26 Sep – night	21.2	0.051	0.065	0.24	0.00	NM	NM	NM	NM	0.09	0.38	0.15	2.71	3.1	
			0.065	0.099	0.17	0.00	NM	NM	NM	NM	0.05	0.29	0.12			
			0.099	0.160	0.86	0.42	0.48	NM	NM	NM	NM	0.1	0.12			0.76
			0.160	0.267	2.02	0.92	0.45	NM	NM	NM	NM	0.26	0.13			1.76
			0.267	0.390	4.46	1.84	0.41	NM	NM	NM	NM	0.37	0.08			4.09
			0.390	0.624	9.34	3.34	0.36	NM	NM	NM	NM	0.64	0.07			8.7
			0.624	0.964	7.76	2.61	0.34	NM	NM	NM	NM	0.66	0.09			7.1
			0.964	1.625	3.64	1.33	0.36	NM	NM	NM	NM	0.52	0.14			3.12
			1.625	2.428	1.11	0.55	0.49	NM	NM	NM	NM	0.22	0.20			0.89
			2.428	4.063	1.1	0.39	0.36	NM	NM	NM	NM	0.43	0.39			0.67
			4.063	6.692	0.64	0.22	0.34	NM	NM	NM	NM	0.18	0.28			0.45
			6.692	10.113	0.28	0.12	0.44	NM	NM	NM	NM	0.09	0.32			0.19
			10.113	30.0	0.24	0.11	0.47	NM	NM	NM	NM	0.06	0.25			0.17
			Fine	29.60	10.99	0.37	NM	NM	NM	NM	NM	2.91	0.10			26.69
			Coarse	2.26	0.85	0.38	NM	NM	NM	NM	0.76	0.34	1.48			
			13	27 Sep – day	13.4	0.047	0.064	0.58	0.16	0.28	0.00	0.00	0.01			0.02
0.064	0.099	0.53				0.15	0.28	0.00	0.00	0.00	0.04	0.08	0.49			
0.099	0.160	1.17				0.42	0.36	0.43	0.37	0.16	0.14	0.1	0.09	1.08		
0.160	0.267	2.75				1.22	0.44	1.19	0.43	0.4	0.15	0.21	0.08	2.54		
0.267	0.389	5.33				2.09	0.39	0.73	0.14	0.56	0.11	0.29	0.05	5.04		
0.389	0.624	7.14				2.27	0.32	0.61	0.09	0.39	0.05	0.7	0.10	6.44		
0.624	0.963	4.12				1.27	0.31	0.63	0.15	0.24	0.06	0.35	0.08	3.77		
0.963	1.624	1.71				0.75	0.44	0.44	0.26	-	0.18	0.11	1.54			
1.624	2.426	0.63				0.30	0.47	0.18	0.29	0.08	0.13	0.05	0.08	0.58		
2.426	4.061	0.89				0.25	0.28	0.33	0.37	0.04	0.04	0	0.00	0.89		
4.061	6.687	0.76				0.25	0.32	0.12	0.16	0.05	0.07	0.04	0.05	0.72		
6.687	10.106	0.24				0.08	0.35	0.02	0.08	0.00	0	0.00	0.00	0.24		
10.106	30.0	0.28				0.09	0.31	0.00	0.00	0.00	0	0.00	0.00	0.28		
Fine	23.96	8.64				0.36	4.21	0.18	1.83	0.08	1.93	0.08	22.04			
Coarse	2.17	0.67				0.31	0.47	0.22	0.09	0.04	0.04	0.02	2.13			

[Title Page](#)
[Abstract](#)
[Introduction](#)
[Conclusions](#)
[References](#)
[Tables](#)
[Figures](#)
[Back](#)
[Close](#)
[Full Screen / Esc](#)
[Printer-friendly Version](#)
[Interactive Discussion](#)


Carbon content of aerosols from the burning of biomass

L. L. Soto-García et al.

Table 1. Continued.

DLPI #	Date	Method used =>		TC	EC _a	EC _a /TC	EGA'		EC _{w572 nm} (extracted)	EC _{w572 nm} (extracted)/TC	LTM''		OC	Aethalometer			
		Volume (m ³)	Size Cut (µm)				EC _a 572 nm (non- extracted)	EC _a 572 nm (non- extracted)/TC			BC _e 880 nm	BC _{e880 nm} / TC		BC _e 571 nm	BC _e 880 nm		
15	28 Sep – day	14.7	0.049	0.064	–	–	–	–	–	–	NM	NM	1.46	1.63			
			0.064	0.099	0.67	0.18	0.27	0.14	0.21	–	–	NM				NM	
			0.099	0.160	1.38	0.48	0.35	0.34	0.25	0.12	0.09	NM				NM	
			0.160	0.267	3.09	1.28	0.41	0.81	0.26	0.38	0.12	NM				NM	
			0.267	0.390	6.4	2.53	0.40	0.41	0.06	0.94	0.15	NM				NM	
			0.390	0.624	9.52	3.46	0.36	1.43	0.15	0.98	0.10	NM				NM	
			0.624	0.964	6.05	2.29	0.38	0.84	0.14	0.62	0.10	NM				NM	
			0.964	1.625	1.83	0.78	0.43	0.47	0.26	0.29	0.16	NM				NM	
			1.625	2.427	1.2	0.48	0.40	0.39	0.33	0.09	0.08	NM				NM	
			2.427	4.062	1.15	0.36	0.31	0.24	0.21	–	–	NM				NM	
			4.062	6.689	0.67	0.20	0.30	0.18	0.27	–	–	NM				NM	
			6.689	10.109	0.42	0.14	0.33	–	–	–	–	NM				NM	
			10.109	30.0	0.41	0.13	0.32	–	–	–	–	NM				NM	
			Fine	30.14	11.48	0.38	4.83	0.16	3.42	0.11	–	–				–	–
			Coarse	2.65	0.83	0.31	0.42	0.16	0.00	0.00	–	–				–	–
25	4 Oct – night	22.0	0.048	0.064	0.33	0.14	0.42	NM	NM	NM	NM	0.16	0.48	0.17	5.58	6.01	
			0.064	0.099	0.57	0.23	0.40	NM	NM	NM	NM	0.09	0.16	0.48			
			0.099	0.160	1.76	0.79	0.45	NM	NM	NM	NM	0.13	0.07	1.63			
			0.160	0.267	4.37	2.05	0.47	NM	NM	NM	NM	0.21	0.05	4.15			
			0.267	0.389	11.08	5.33	0.48	NM	NM	NM	NM	0.24	0.02	10.84			
			0.389	0.624	22.77	11.13	0.49	NM	NM	NM	NM	1.01	0.04	21.76			
			0.624	0.964	15.91	6.98	0.44	NM	NM	NM	NM	0.96	0.06	14.95			
			0.964	1.624	6.44	2.45	0.38	NM	NM	NM	NM	0.59	0.09	5.85			
			1.624	2.426	1.27	0.59	0.47	NM	NM	NM	NM	0.57	0.45	0.71			
			2.426	4.061	2.23	0.72	0.32	NM	NM	NM	NM	0.41	0.18	1.82			
			4.061	6.688	1.7	0.55	0.32	NM	NM	NM	NM	0	0.00	1.7			
			6.688	10.107	0.79	0.29	0.37	NM	NM	NM	NM	0.16	0.20	0.63			
			10.107	30.0	0.25	0.13	0.51	NM	NM	NM	NM	0.14	0.56	0.11			
			Fine	64.5	29.69	0.46	–	–	–	–	–	–	3.96	0.06			60.54
			Coarse	4.97	1.69	0.34	–	–	–	–	–	–	0.71	0.14			4.26
Average			Fine	44.26	18.06	0.40	5.23	0.15	3.17	0.09	3.11	0.07	43.96	3.21	3.59		
			STDEV	18.33	9.10	0.04	1.27	0.03	1.23	0.02	0.80	0.02	18.25	1.86	1.99		
			Coarse	3.38	1.11	0.34	0.39	0.18	0.05	0.03	0.48	0.14	3.04	NM	NM		
			STDEV	1.91	0.56	0.04	0.10	0.03	0.05	0.02	0.34	0.12	1.90	–	–		

Title Page

Abstract

Introduction

Conclusions

References

Tables

Figures

⏪

⏩

◀

▶

Back

Close

Full Screen / Esc

Printer-friendly Version

Interactive Discussion



Carbon content of aerosols from the burning of biomass

L. L. Soto-García et al.

Title Page

Abstract

Introduction

Conclusions

References

Tables

Figures

◀

▶

◀

▶

Back

Close

Full Screen / Esc

Printer-friendly Version

Interactive Discussion



Table 2. TC concentration results from the DLPI and different filter systems. These samples were collected during the dry period of the LBA-SMOCC campaign. All concentrations are given in $\mu\text{g m}^{-3}$.

Sample ^a	DLPI (UPR)	R2.5WW (UGent)	Carbon Monitor (USP)	HVDS (MPIC)	1HVDS (UGent)	2HVDS (UGent)
15 Sep N	17.4	16.58	14.85	14.06	16.67	15.86
16 Sep N	53.9	51.21	48.43	44.14	52.34	48.98
17 Sep N	67.0	51.89	64.58	30.72	57.65	51.06
23 Sep N	29.9	29.64	34.79	34.16	36.21	34.35
24 Sep D	16.1	22.55	21.85	20.92	20.84	21.13
25 Sep D	81.2	64.00	57.23	–	69.65	63.96
26 Sep D	50.0	33.85	34.06	31.98	31.20	32.50
27 Sep D	27.6	16.41	15.68	14.75	17.89	15.67
29 Sep	7.4	7.98	6.40	6.96	7.77	7.00
30 Sep	13.2	9.36	7.20	8.88	9.79	8.82
3 Oct D	15.6	17.25	22.85	16.44	18.71	16.87
3 Oct N	57.9	47.90	58.04	51.83	57.57	50.11
4 Oct D	30.9	27.48	24.24	24.73	28.81	26.79
4 Oct N	58.4	50.06	60.65	51.83	60.70	54.41
6 Oct D	30.9	23.59	24.66	–	24.65	22.15
7 Oct N	27.9	26.54	27.15	–	27.41	24.36
Day	36.1	29.31	28.65	21.77	30.25	28.44
Average						
STDEV	23.0	16.42	13.72	6.92	18.08	16.69
Night	44.6	39.12	44.07	37.79	44.08	39.87
Average						
STDEV	19.1	14.51	18.87	14.57	17.33	15.12

^a The samples collected between 15 September–27 September and 3 October–7 October are from 12-h periods; the date indicates the starting date of sampling, D and N represent day and night samples, respectively. The samples from 29–30 September were collected over 24-h periods.

Carbon content of aerosols from the burning of biomass

L. L. Soto-García et al.

Table 3. Comparison of TC and EC_a measurements by two different laboratories (University of Gent [Gent] and Desert Research Institute [DRI]) using the TOT and TOR techniques. All concentrations are given in $\mu\text{g m}^{-3}$.

Sample ^a	TC		EC _a (TOR)		EC _a (TOT)		EC _a Ratio TOR _{DRI} / TOT _{DRI}	EC _a Ratio TOR _{DRI} / TOT _{Gent}
	DRI	Gent	DRI	DRI	Gent			
18 Sep D	21.4	28.1	3.22	1.83	0.80	1.76	4.04	
18 Sep N	58.3	54.2	5.67	3.10	2.10	1.83	2.70	
19 Sep D	27.4	40.0	2.63	0.15	0.76	17.10	3.47	
19 Sep N	74.7	78.5	9.62	5.55	2.18	1.73	4.40	
20 Sep N	76.1	84.1	6.16	0.32	2.01	19.44	3.06	
13 Oct D	8.6	12.1	1.37	0.71	0.36	1.93	3.75	
13 Oct N	12.4	13.4	2.41	1.28	0.67	1.88	3.61	
16 Oct	7.2	7.4	1.27	0.63	0.35	2.03	3.65	
17 Oct	13.4	13.6	2.22	1.09	0.50	2.03	4.48	
18 Oct	13.3	14.1	2.12	0.95	0.57	2.23	3.72	
Average	31.3	34.5	3.67	1.56	1.03	1.93	3.69	

^a The samples collected between 18 September and 13 October are for 12-h periods; the date indicates the starting date of sampling, D and N represent day and night samples, respectively. The samples from 16–18 October were collected over 24-h periods.

Title Page

Abstract

Introduction

Conclusions

References

Tables

Figures

◀

▶

◀

▶

Back

Close

Full Screen / Esc

Printer-friendly Version

Interactive Discussion



Carbon content of aerosols from the burning of biomass

L. L. Soto-García et al.

Title Page

Abstract

Introduction

Conclusions

References

Tables

Figures

◀

▶

◀

▶

Back

Close

Full Screen / Esc

Printer-friendly Version

Interactive Discussion



Table 4. Average of the size-resolved Ångström exponent, α , for samples non-extracted (α) and extracted with water (α_x) using a thermal-optical analyzer (TOA) at 100°C.

D_p (μm)	Ångström exponent, α	Ångström exponent, α_x
0.05–0.1	1.8*	–
0.10–0.16	2.0	0.7*
0.16–0.27	2.8	1.6
0.37–0.39	3.9	1.2*
0.39–0.62	3.1	1.5
0.62–0.97	2.6	1.1
0.97–1.6	2.1	1.3*

The average of the Ångström exponent presented here are for three samples. The ones marked by * are measurement for only one sample.

Carbon content of aerosols from the burning of biomass

L. L. Soto-García et al.

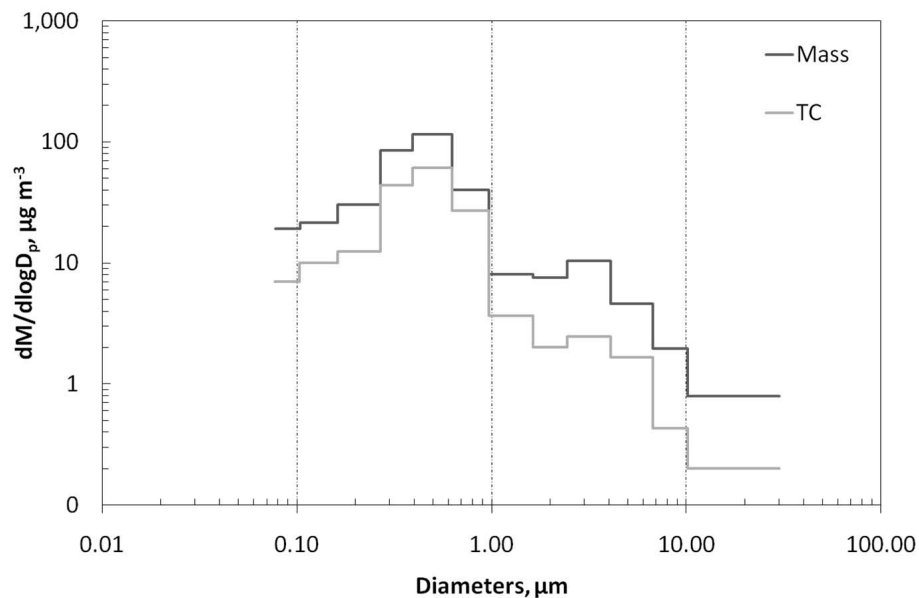


Fig. 1. Average particulate mass and TC size distributions during the dry period. The size distribution for the mass and TC concentrations are the average for all samples collected on aluminum foil substrates during the dry period ($n = 6$).

Title Page

Abstract

Introduction

Conclusions

References

Tables

Figures

◀

▶

◀

▶

Back

Close

Full Screen / Esc

Printer-friendly Version

Interactive Discussion



Carbon content of aerosols from the burning of biomass

L. L. Soto-García et al.

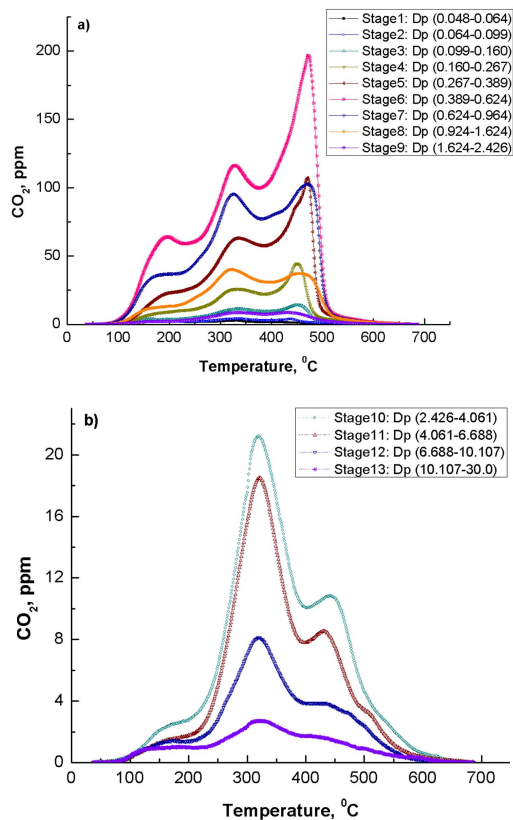


Fig. 2. Typical thermograms determined by EGA showing the thermal characteristics of size-resolved aerosol samples from biomass burning for one set of samples (DLPI#25): evolved carbon (CO_2 , ppm) versus temperature. There are three distinguishable peaks indicating different volatilities and/or reactivities. **(a)** Fine particles. The last peak is dominant (less volatile and highly refractory). **(b)** Coarse particles. The first two peaks are more significant.

[Title Page](#)
[Abstract](#)
[Introduction](#)
[Conclusions](#)
[References](#)
[Tables](#)
[Figures](#)
[◀](#)
[▶](#)
[◀](#)
[▶](#)
[Back](#)
[Close](#)
[Full Screen / Esc](#)
[Printer-friendly Version](#)
[Interactive Discussion](#)


Carbon content of aerosols from the burning of biomass

L. L. Soto-García et al.

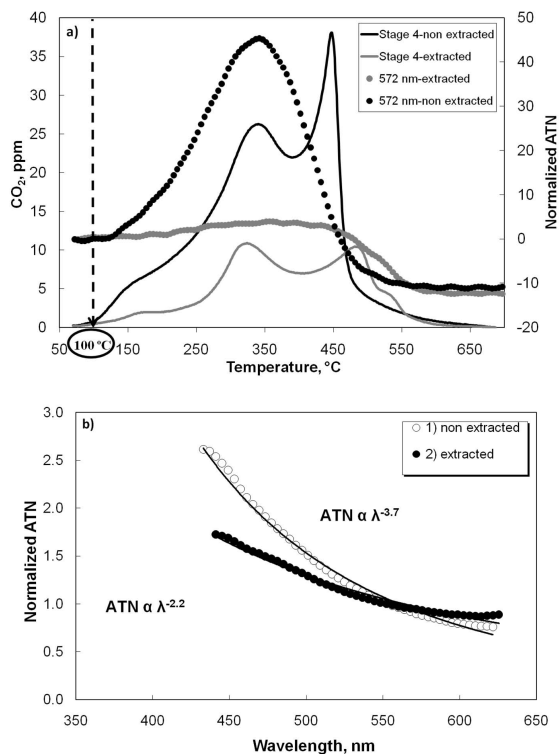


Fig. 3. (a) Thermal-optical analysis of quartz fiber filter samples (water extracted and non-extracted), (b) The spectral attenuation (normalized ATN) measured at 100°C for DLPI#11-stage 4 (D_p : 0.2–0.3 μm).

Title Page

Abstract

Introduction

Conclusions

References

Tables

Figures

◀

▶

◀

▶

Back

Close

Full Screen / Esc

Printer-friendly Version

Interactive Discussion

Carbon content of aerosols from the burning of biomass

L. L. Soto-García et al.

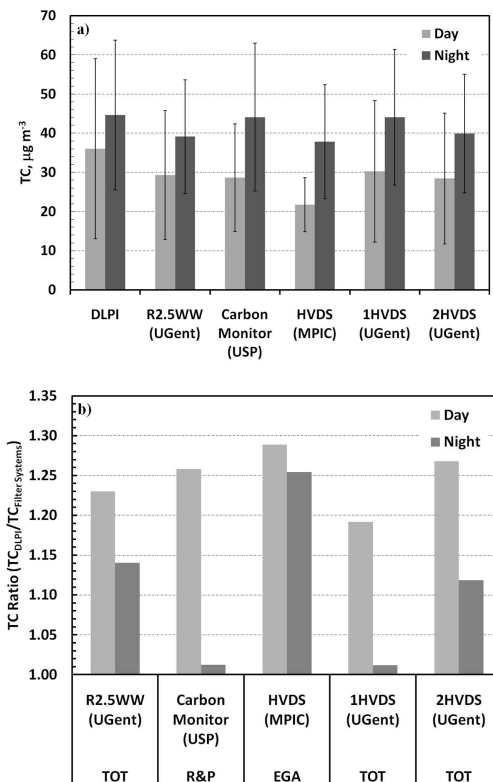


Fig. 4. (a) TC concentration averages ($D_p < 2.5 \mu\text{m}$) for DLPI (UPR) and R2.5WW (UGent), carbon monitor (USP), HVDS (MPIC), 1HVDS (UGent), 2HVDS (UGent) together with the standard deviation bars for day and night time samples. The number of samples used for each system were: DLPI (UPR) – $n = 3$; R2.5WW (UGent), carbon monitor (USP), HVDS (MPIC), 1HVDS (UGent), 2HVDS (UGent) – $n = 37$. **(b)** TC concentration ratio of the different filter systems relative to the DLPI ($D_p < 2.5 \mu\text{m}$) for day and night time.

Title Page

Abstract Introduction

Conclusions References

Tables Figures

◀ ▶

◀ ▶

Back Close

Full Screen / Esc

Printer-friendly Version

Interactive Discussion



Carbon content of aerosols from the burning of biomass

L. L. Soto-García et al.

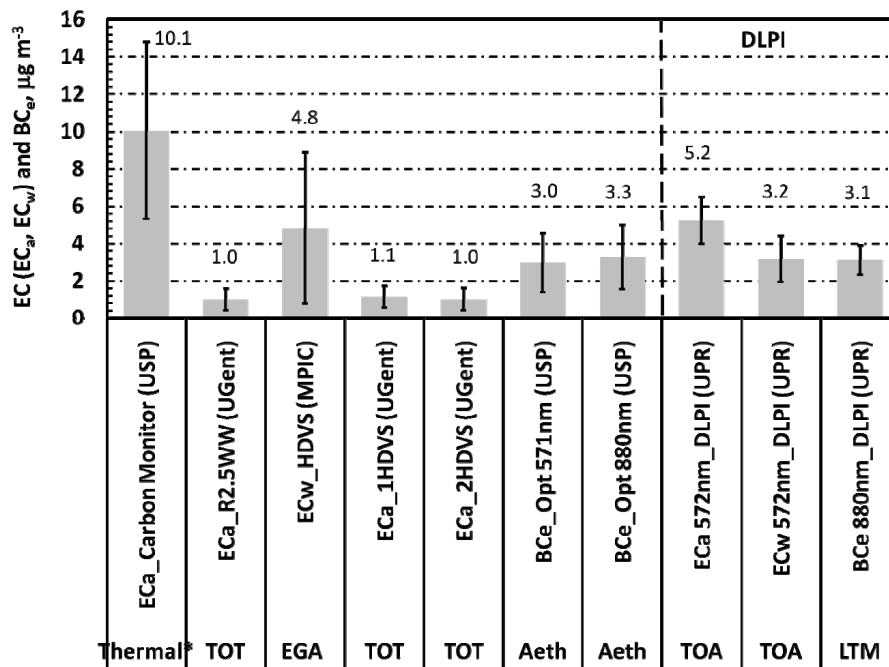


Fig. 5. (a) Comparison of EC (EC_a and EC_w) and BC_e averages for $D_p < 2.5 \mu\text{m}$ using the carbon monitor, HVDS (MIPIC), 1HVDS (UGent), 2HVDS (UGent), Aethalometer (at 571 nm and 880 nm), and the DLPI together with the standard deviation bars. Only for the Aethalometer the $D_p < 10 \mu\text{m}$. EC_a refers to non-extracted thermal samples and EC_w refers to water extracted samples using thermal, TOA and TOT methods. BC_e _Opt 571 nm and BC_e _Opt 880 nm refers to the species measured by the aethalometer at two wavelengths mentioned. BC_e 880 nm_DLPI refers to the species measured by the light transmission method at 880 nm.

Carbon content of aerosols from the burning of biomass

L. L. Soto-García et al.

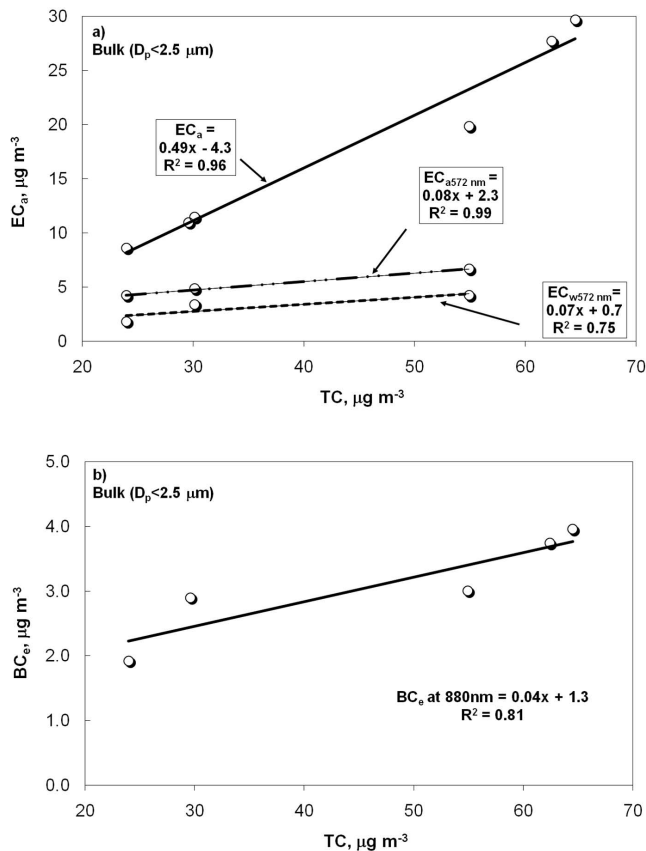


Fig. 6. (a) EC_a (EC_a , $EC_{a572 \text{ nm}}$ (non-extracted), $EC_{w572 \text{ nm}}$ (extracted)) and (b) $BC_{e880 \text{ nm}}$ as a function of TC concentrations measured for the fine aerosol ($D_p < 2.5 \mu\text{m}$).

Title Page

Abstract Introduction

Conclusions References

Tables Figures

◀ ▶

◀ ▶

Back Close

Full Screen / Esc

Printer-friendly Version

Interactive Discussion



Carbon content of aerosols from the burning of biomass

L. L. Soto-García et al.

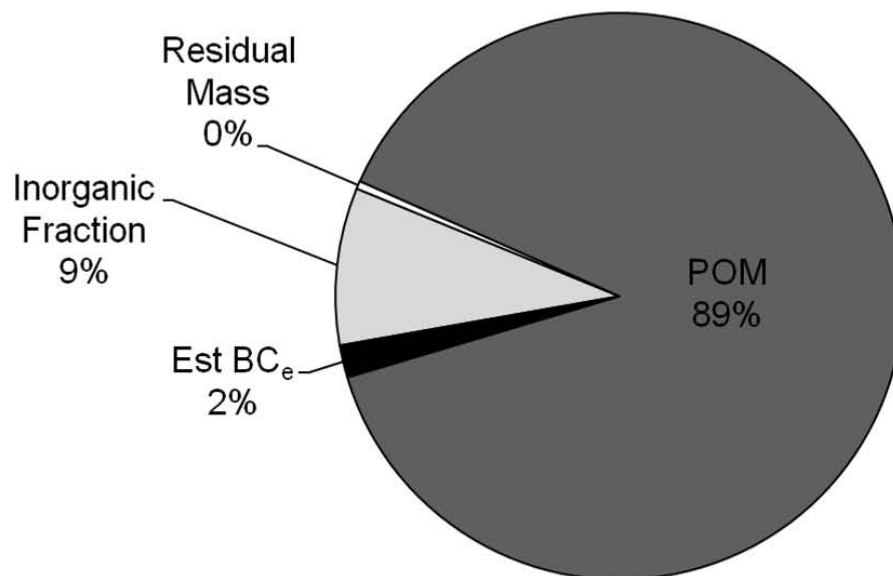


Fig. 7. Carbonaceous aerosol composition for the fine fraction ($D_p < 2.5, \mu\text{m}$) during the dry season. POM (particulate organic material) has been calculated from $[\text{TC} - \text{BC}_e] \cdot 1.8$. The inorganic fraction was calculated by adding the average of all individual species measured. BC_e has been estimated by using a regression line of $\text{BC}_{e880 \text{ nm}}$ vs. TC ($y = 0.02x + 0.51$; $r^2 = 0.86$; $n = 5$).

[Title Page](#)[Abstract](#)[Introduction](#)[Conclusions](#)[References](#)[Tables](#)[Figures](#)[◀](#)[▶](#)[◀](#)[▶](#)[Back](#)[Close](#)[Full Screen / Esc](#)[Printer-friendly Version](#)[Interactive Discussion](#)

Carbon content of aerosols from the burning of biomass

L. L. Soto-García et al.

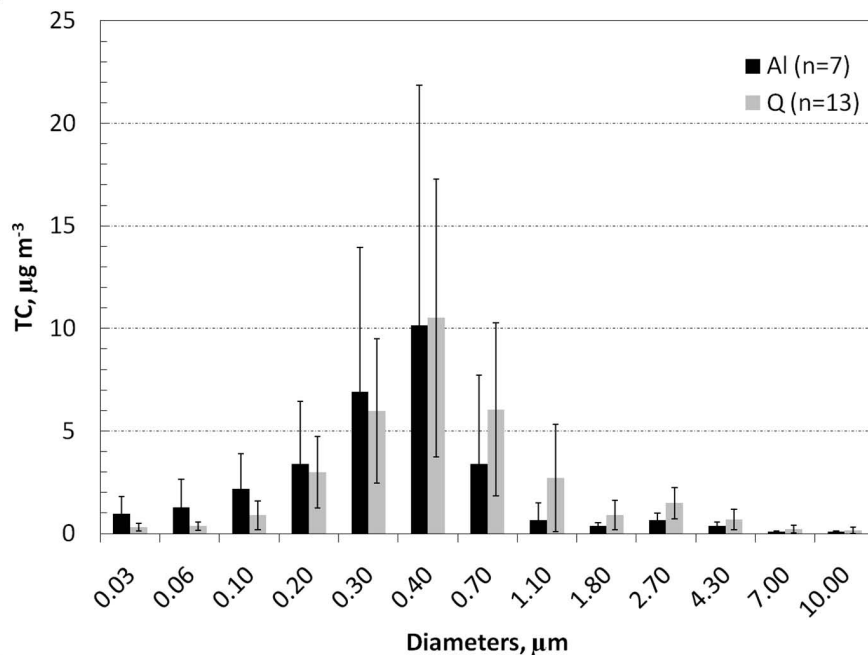


Fig. 8. Size-resolved averaged TC mass concentration when using aluminum substrates ($n = 7$) and quartz fiber filters ($n = 13$) for the DLPI sampler.

[Title Page](#)[Abstract](#)[Introduction](#)[Conclusions](#)[References](#)[Tables](#)[Figures](#)[◀](#)[▶](#)[◀](#)[▶](#)[Back](#)[Close](#)[Full Screen / Esc](#)[Printer-friendly Version](#)[Interactive Discussion](#)

Carbon content of aerosols from the burning of biomass

L. L. Soto-García et al.

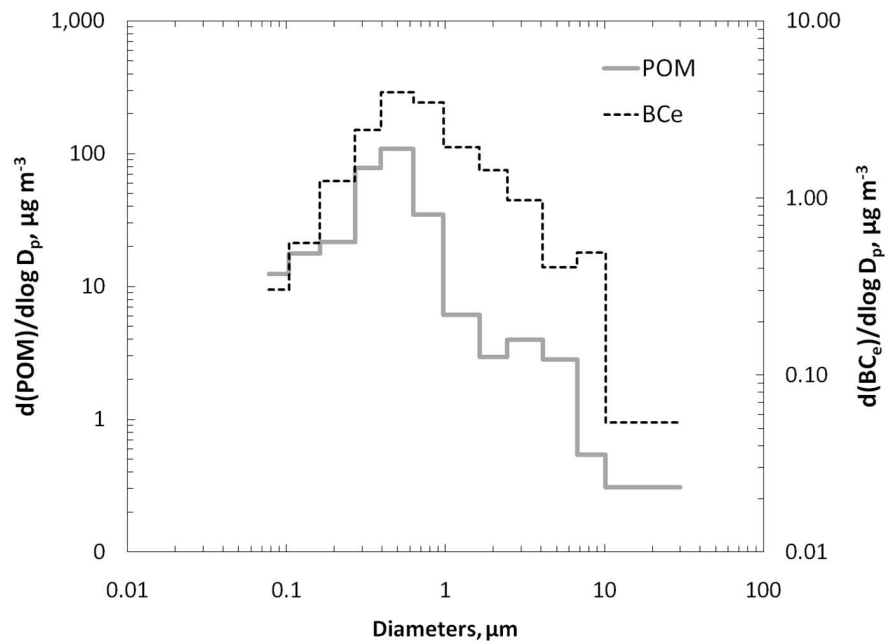


Fig. 9. Size distribution of the average POM and BC_e concentrations. POM (particulate organic material) has been calculated from $[\text{TC}-\text{BC}_e]\cdot 1.8$.

Title Page

Abstract

Introduction

Conclusions

References

Tables

Figures

◀

▶

◀

▶

Back

Close

Full Screen / Esc

Printer-friendly Version

Interactive Discussion



Carbon content of aerosols from the burning of biomass

L. L. Soto-García et al.

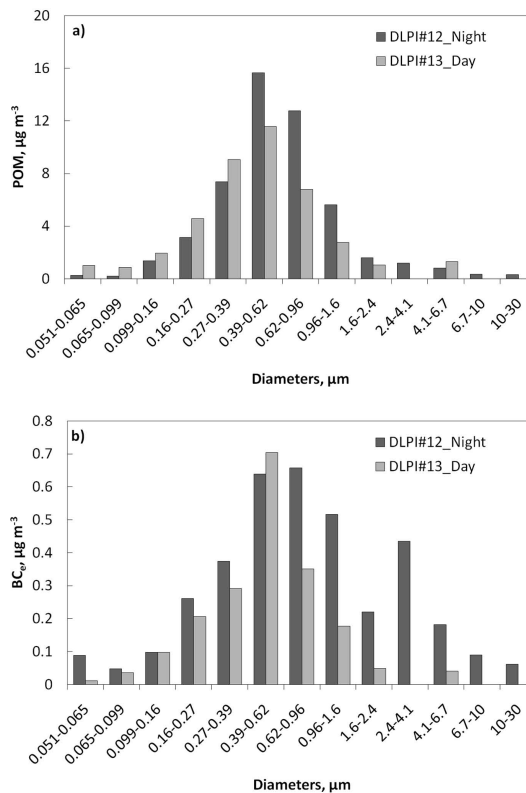


Fig. 10. Size-resolved nighttime (DLPI#12) and daytime (DLPI#13) **(a)** POM and **(b)** BC_e concentrations for selected samples. These examples show the diurnal variation of the size-resolved POM and BC_e during the SMOCC-2002 campaign.

[Title Page](#)
[Abstract](#)
[Introduction](#)
[Conclusions](#)
[References](#)
[Tables](#)
[Figures](#)
[◀](#)
[▶](#)
[◀](#)
[▶](#)
[Back](#)
[Close](#)
[Full Screen / Esc](#)
[Printer-friendly Version](#)
[Interactive Discussion](#)
